ChemMedChem

Chemistry Europe
European Chemical Societies Publishing

Accepted Article

Title: Synthesis and pharmacological evaluation of σ2 receptor ligands based on a 3-alkoxyisoxazole scaffold: potential antitumor effects against osteosarcoma

Authors: Jun-Jie Shi, Kun-Hang Jia, Hao Sun, Hendra Gunosewoyo, Fan Yang, Jie Tang, Jian Luo, and Lifang Yu

To be cited as: *ChemMedChem* 10.1002/cmdc.202000461

Link to VoR: https://doi.org/10.1002/cmdc.202000461

WILEY-VCH

Synthesis and pharmacological evaluation of σ2 receptor ligands based on a 3-alkoxyisoxazole scaffold: potential antitumor effects against osteosarcoma

Jun-Jie Shi,[†,#] Kun-Hang Jia,[§,#] Hao Sun,[†] Hendra Gunosewoyo,[⊥] Fan Yang,[†] Jie Tang,[□] Jian Luo,[§] and Li-Fang Yu[*,†]

[†]Shanghai Engineering Research Center of Molecular Therapeutics and New Drug Development, School of Chemistry and Molecular Engineering, East China Normal University, 3663 North Zhongshan Road, Shanghai 200062, China

[§]Shanghai Key Laboratory of Regulatory Biology, Institute of Biomedical Sciences and School of Life Sciences East China Normal University, 500 Dongchuan Road, Shanghai 200241, China

[⊥]School of Pharmacy and Biomedical Sciences, Faculty of Health Sciences, Curtin University, Bentley, Perth, WA 6102, Australia

[□]Shanghai Key Laboratory of Green Chemistry and Chemical Process, School of Chemistry and Molecular Engineering, East China Normal University, 3663 North Zhongshan Road, Shanghai 200062, China

Graphical Abstract

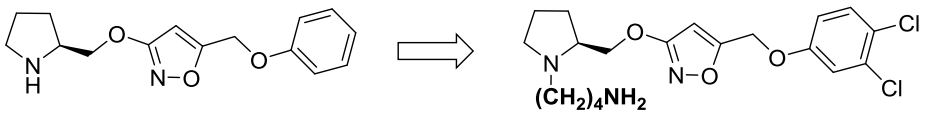

10
K_i, σ1 = 4.1 nM
K_i, σ2 = 1312 nM
no activity against 143B osteosarcoma cells

51
σ1: 78% inhibition at 10 μM
K_i, σ2 = 7.9 nM
inhibit the proliferation (IC_{50} = 0.89 μM) and colony-formation ability of 143B osteosarcoma cells

Abstract

Since the initial discovery as nicotinic acetylcholine receptor ligands, the 3-alkoxyisoxazole scaffold has now been shown as a versatile platform for the development of potent σ1 and σ2 receptor ligands. Herein we report a further SAR exploration on the 3-alkoxyisoxazole scaffold with the aim of obtaining potent σ2 receptor ligands. Various substitutions on the benzene ring and the basic amino regions resulted in a total of 21 compounds that were tested for their binding affinities to σ2 receptor. In particular, compound **51** was identified as one of the most potent σ2 ligands within the series with a K_i value of 7.9 nM, and demonstrated potent anti-proliferative effects on the both osteosarcoma cell lines 143B and MOS-J (IC_{50} values of 0.89 and 0.71 μM, respectively), compared to siramesine (IC_{50} values of 1.81 and 2.01 μM). Moreover, compound **51** inhibited the clonal formation of the osteosarcoma 143B cells at 1 μM concentration, corresponding to half the dose required of siramesine for similar effects. The general cytotoxicity profile of compound **51** was assessed in a number of normal cell lines, including HaCaT, HAF, and LO2 cells. Furthermore, FACS analysis showed that compound **51** likely inhibits the osteosarcoma cell growth by disruption of the cell cycle and promotion of cell apoptosis.

Keywords: σ2 receptor, 3-alkoxyisoxazoles, osteosarcoma, antiproliferative effects, colony formation, cytotoxicity, siramesine

Introduction

The sigma (σ) receptors were originally classified by Martin *et al.* in 1976 as an additional subtype of opioid receptors family [1]. However, later it was found that the pharmacological effects produced

by SKF-10047 failed to be antagonized by naloxone [2]. Since then there has been subsequent confusion in the literature, associating the σ receptors with the PCP binding site of NMDA receptor. Currently, σ receptors are considered a unique entity with no homology to opioid receptors or other mammalian proteins [3], and two distinct subtypes termed σ1 and σ2 have been identified [4]. Both of these receptors have been implicated in the pathophysiology of various neurological disorders and cancer [5]. The σ1 receptor contains 223 amino acids with two transmembrane domains [6] and the crystal structure of the human σ1 receptor in complex with two chemically divergent ligands was first reported in 2016 [7]. The σ1 receptor regulates the activity of a large number of cellular proteins [8] including ion channels, G protein-coupled receptors (GPCRs), transcription factors, endoplasmic reticulum (ER) chaperone protein BiP, as well as acting as a molecular chaperone to repair misfolded proteins [9]. Activation of the σ1 receptor results in the transport of cholesterol, ceramides, and essential amino acids that are necessary for cell growth and reproduction, along with the synthesis of various growth factors involved in neuronal growth [10]. Very recently, choline has been identified as the endogenous ligand for σ1 receptor [11].

In 1990, Hellewell *et al.* first reported a distinct population of σ receptors that were different to those from guinea pig brain, which was then termed the σ2 receptor [12]. It comprises of 18-21 kDa membrane protein [12], which are highly expressed in the liver, kidney, and proliferating tumor tissues [5a, 13]. Similar to the σ1 story, the identification of σ2 receptor has taken many twists and turns. At the outset, σ2 receptor was considered as a histone binding protein [14]. In 2011, progesterone receptor membrane component 1 (PGRMC1) protein complex, a potential therapeutic target for inhibiting tumorigenesis [15], was thought to be the binding site of σ2 receptor as overexpression and

knockdown of the PGRMC1 protein results in a subsequent increase and decrease, respectively, of the σ2 selective radioligand binding [16]. However, recent studies have suggested that PGRMC1 and σ2 receptor are two different molecular entities as evidenced by fluorescent labeling experiments [17]. In 2017, Alon *et al.* identified TMEM97, which is an endoplasmic reticulum-resident transmembrane protein that regulates the sterol transporter NPC1. It was revealed that Asp 29 and Asp 56 are essential amino acid residues for ligand recognition [18].

Even before its identification and molecular cloning, the σ2 receptor has been long considered to be a potential therapeutic target for cancer. From the initial proposal as reliable biomarkers of tumors [13b], a variety of structurally diverse σ2 receptor ligands have been studied in different tumors, including pancreatic cancer, breast cancer, metastatic melanoma, and neuroblastoma, with siramesine (**1**, K_i, σ1 = 17.0 nM, K_i, σ2 = 0.12 nM), SV-119 (**2**, K_i, σ1 = 1417 nM, K_i, σ2 = 5.2 nM), WC-26 (**4**, K_i, σ1 = 1436 nM, K_i, σ2 = 2.6 nM), and RHM-138 (**5**, K_i, σ1 = 544 nM, K_i, σ2 = 12.3 nM) utilized in preclinical trials (**Figure 1**) [19]. Although the exact roles of σ2 receptor in these tumors remain unclear, development of selective σ2 radioligands in tandem with fluorescent labeling have led to a better understanding of the cellular actions and biological pathways associated with the σ2 receptor. For example, SW-43 (**3,** K_i, σ2 = 18 nM), a fluorescently labeled σ2 receptor ligand, mediated pancreatic cancer cells death by lysosomal membrane permeabilization, while PB-28 (**6**, K_i, σ1 = 13.0 nM, K_i, σ2 = 0.28 nM) could induce cell death via mitochondrial superoxide production and caspase activation in pancreatic cancer (**Figure 1**) [19a, 20]. For human SK-N-SH neuroblastoma cells, CM-572 (**7,** K_i, σ1 > 10 μM, K_i, σ2 = 14.6 nM) induced an immediate dose-dependent increase in cytosolic calcium concentration，and the newer benzoxazole and benzothiazole derivatives were

reported to inhibit the viability of breast cancer cells [19h, 21]. A study with fluorescent probe K05-138 (**8**, K_i, σ1 = 1100 nM, K_i, σ2 = 45 nM) suggests that σ2 ligands are internalized by an endocytotic pathway in breast cancer cells [22]. Other potential antitumour mechanisms have also been reported in conjunction with these σ2 receptor ligands, including reactive oxygen species (ROS), P-glycoprotein, DNA fragmentation, proline rich acidic protein 1 (PRAP-1) cleavage, among others. [19c, 23]. Moreover, σ2 ligands have also been proposed to be effective for imaging the proliferation status in tumors as potential diagnostic tools for cancer [24], with [18F] ISO-1 (**9**，K_i, σ1 = 330 nM, K_i, σ2 = 7.0 nM) currently being evaluated in the phase I clinical trial as a potential positron emission tomography (PET) marker [24d]. Synergistic or potentiating effects of σ2 receptor ligand with an anticancer agent, as exemplified by SV-119 combined with gemcitabine or paclitaxel, was also demonstrated to stabilize pancreatic cancer progression in rodents [19b, 25]. Other studies also showed that σ2 receptor ligands could be used in combination with other antitumor agents to selectively target the cancer cells [26]. In addition, σ2 receptor ligands have also been associated with the modulation of metabolic stimulation, neuralgia, and anticonvulsant effects [11, 27].

10.1002/cmdc.202000461

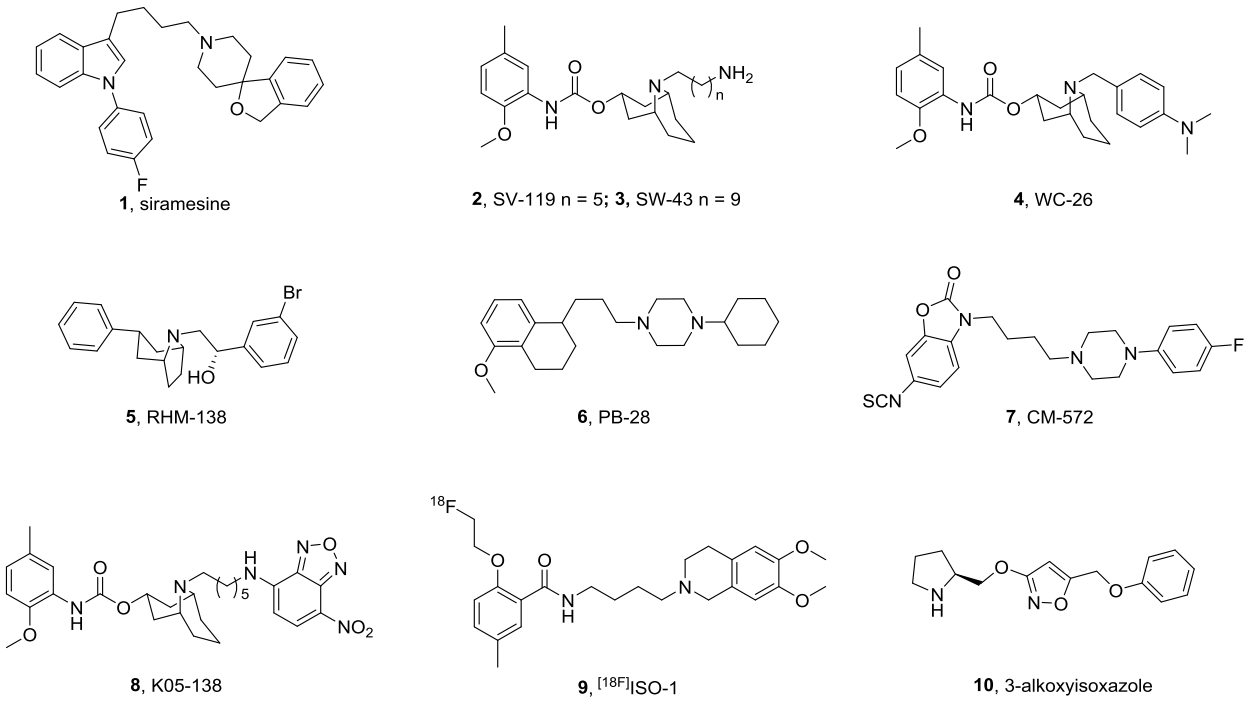

Figure 1. Structures of selected σ2 receptor ligands.

Our previous work in the development of σ receptor ligands have identified 3-alkoxyisoxazole **10** scaffold as σ1 receptor ligands with high affinity and selectivity (K_i, σ1 = 4.1 nM, K_i, σ2 = 1312 nM) [28]. This compound was originally obtained during our investigation of the α4β2 nicotinic receptor ligands through a comparative pharmacophore analysis between the nicotinic receptor and the σ1 receptor. Since then, we have identified σ1 ligands with good pharmacokinetic properties and excellent brain/plasma ratio, one of which has been shown to possess significant analgesic effects in formalin-induced mouse inflammatory pain model [29]. Subsequently, incorporation of a cyclobutylaminoethoxy side-chain on the isoxazole afforded highly potent and selective σ1 receptor ligands that demonstrate neurite outgrowth activity on the N1E-115 neurite cell model [30]. In the present study, we report our structure-activity relationship (SAR) findings on the 3-alkoxyisoxazole derivatives that possess moderate to good σ2 affinities (K_i values in the range of 1.8 nM to 1008 nM)

and their potential antitumor activities in osteosarcoma cells.

Results and Discussion

Chemistry

As described previously [29], the key intermediate **12** was synthesized starting from the commercially available dimethyl 2-butynedioate **11** in 4 steps, involving sequential [2+3] cycloaddition, Mitsunobu reaction, reduction, and iodination (Scheme 1). Compounds **13-25** were synthesized via substitution reaction of iodide **12** with various phenols under basic condition, followed by deprotection of the Boc group in the presence of either hydrochloric acid or trifluoroacetic acid (TFA). Compounds **23-25** underwent reductive amination with formaldehyde to give the tertiary amines **26-28**. Compound **30**, which differs in the position of the secondary amine, was synthesized in a similar manner to compound **13** using compound **29** as the starting material.

Scheme 1.

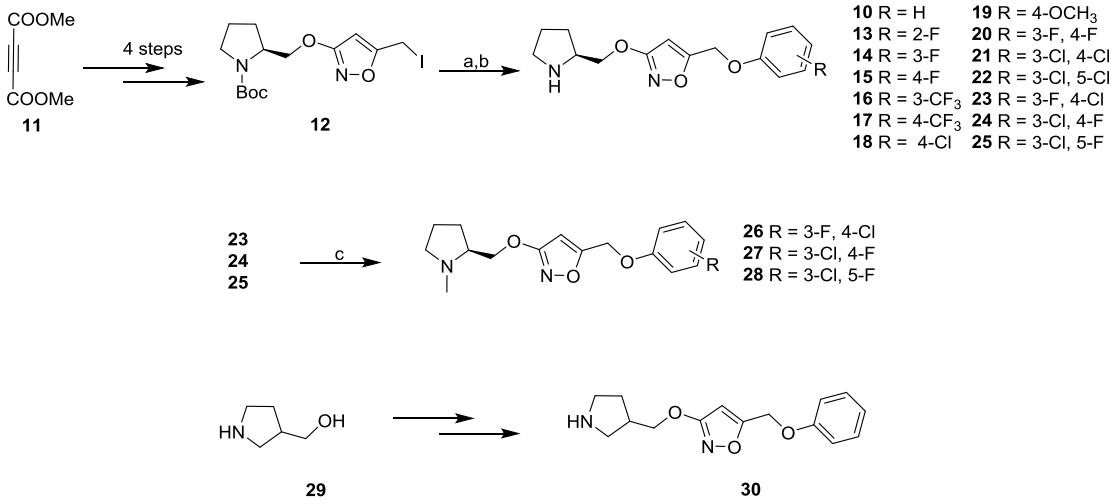

Reagents and conditions: (a) substituted phenol, K_2CO_3, DMF, rt; (b) HCl, EtOAc, rt or TFA, CH_2Cl_2, rt; (c) HCHO, $NaBH_4$, CF_3CH_2OH, 40 ℃.

10.1002/cmdc.202000461

A series of *N*-cycloalkyl substituents were introduced instead of the original pyrrolidine ring to afford the *N*-cycloalkylaminoethoxyisoxazole derivatives **35-41** (Scheme 2). In a similar manner to the synthesis of compounds **13-25** (Scheme 1), ethanolamine **31** and *N*-methylethanolamine **32** underwent sequential Mitsunobu reaction with 3-hydroxyisoxazole-5-carboxylic acid methyl ester, lithium borohydride reduction, and iodination to give the iodides **33** and **34** [30]. Substitution reaction with the appropriate phenols under basic conditions, Boc deprotection with HCl, and reductive amination with the corresponding cyclic ketones provided compounds **35-41**. Alkaline hydrolysis of ester **41** followed by amide coupling with dimethylamine using HATU in DMF as a solvent afforded amide **42.** Reduction with lithium aluminum hydride formed the final diamine **43**.

In turn, a series of *N*-(aminoalkyl) substituents were attached to the pyrrolidine site to give the isoxazoles **48-51** as described in Scheme 2. Iodoaminoalkanes **46** and **47** were first prepared from the corresponding aminoalcohols **44** and **45**, respectively, via Boc protection and iodination using Appel condition. Substitution reaction of iodoaminoalkanes **46-47** with compounds **10, 16,** and **21** gave the desired final compounds **48-51**. All the final products **10**, **13-28**, **30**, **35-43**, and **48-51** were obtained either as hydrochloride or trifluoroacetate salts with the exception of free bases **26-28** and **42**.

Scheme 2.

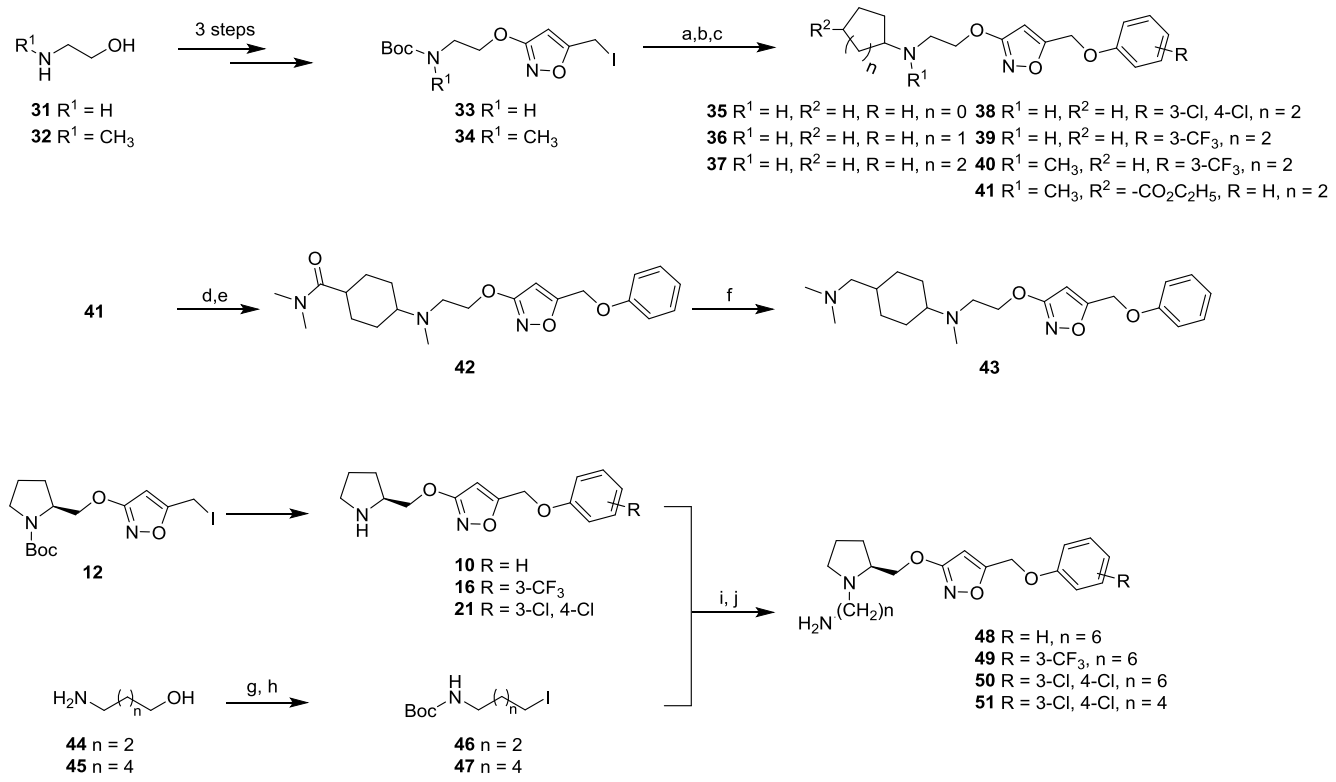

Reagents and conditions: (a) phenol or substituted phenol, K_2CO_3, DMF, rt; (b) HCl, EtOAc, rt, then aqueous NaOH solution; (c) cyclic ketone, $NaBH_3CN$, CH_3CO_2H, CH_3OH, rt; (d) NaOH, THF/H_2O, rt; (e) dimethylamine hydrochloride, 1-[bis(dimethylamino)methylene]-1*H*-1,2,3-triazolo[4,5-*b*]pyridinium 3-oxid hexafluorophosphate (HATU), *N*, *N*-diisopropylethylamine, DMF, rt; (f) $LiAlH_4$, THF, 0 ℃ to rt; (g) di-*tert* butyl dicarbonate, K_2CO_3, THF/H_2O, rt; (h) I_2, PPh_3, imidazole, CH_2Cl_2, 0 ℃ to rt; (i) K_2CO_3, DMF, rt or heat to 60 ℃; (j) HCl/EtOAc, rt.

Radioligand Binding Studies

In vitro binding affinities of compounds **10**, **13-28**, **30**, **35-40**, **42**, **43**, and **48-51** at σ1 andσ2 receptor were determined by the National Institute of Mental Health's Psychoactive Drug Screening Program

(NIMH PDSP) using the standard [^{3}H]-(+)-pentazocine and [^{3}H] DTG binding assay with rat brain homogenate and PC12 cells respectively(Tables 1 and 2). Firstly, keeping the 2-pyrrolidine moiety intact, the effects of monosubstitution on the phenolic ether region were explored including fluoro (**13-15**), trifluoromethyl (**16-17**), chloro (**18**) and methoxy (**19**) groups, to investigate the optimal electronic requirements for enhanced σ2 affinity. The *o*-fluoro substituted compound **13** had approximately 3.3-fold increase on the σ2 receptor affinity vs the parent compound **10**, while the *m*-fluoro substituted (**14**) and *p*-fluoro substituted (**15**) analogues had 5-fold and 3-fold increase respectively, indicating that *m*-substitution was preferred for optimal σ2 receptor affinity. Introduction of a trifluoromethyl group at the *p*-position (**17**) resulted in a 14-fold increase in σ2 receptor affinity (K_i = 91.7 nM) compared to **10**. The *p*-chloro (**18**) and *p*-methoxy (**19**) analogues showed 9-fold and 2-fold increase, with σ2 K_i values of 139 and 675 nM, respectively. Compared to **17**, the trifluoromethyl substitution at the *m*-position resulted in a slightly more potent compound **16** with a K_i value of 88 nM. Within the tested analogues **13-19**, affinity at σ2 receptor was improved upon monosubstitution with an electron withdrawing group (EWG). Following this observation, various EWG disubstitutions (fluoro and chloro groups) were introduced to the phenolic ether region to further probe the electronic requirements on the benzene ring. The *m*, *p*-difluoro substituted compound **20** retained a similar affinity at σ2 receptor (K_i, σ2 = 373 nM) compared to the monofluoro analogues **13-15**. On the other hand, the *m*, *p*-dichloro (**21**) and *m*, *m*-dichloro (**22**) analogues showed higher σ2 receptor binding affinities than the monochloro analogue **18**, with approximately 29-fold and 25-fold increase on the σ2 affinity relative to parent compound **10**. Simultaneous introduction of fluorine and chlorine at the *m*- and *p*-positions (**23-25**; K_i, σ2 = 128 nM, 202 nM, and 226 nM, respectively) resulted in compounds with higher affinity than the difluoro

analogue **20** but lower affinity than the dichloro substituted compounds **21** (K_i, σ2 = 45 nM) and **22** (K_i, σ2 = 52 nM), therefore dichloro substitution was proved to be superior for σ2 binding affinity compared to the monochloro substitution. We also examined the effect of alkyl substitution on the free nitrogen atom of pyrrolidine ring to probe its ionic/hydrogen bonding requirements. Methylation of the nitrogen atom of the pyrrolidine (compounds **26-28**) generally maintained the σ2 binding affinites, with K_i values ranging from 71.3 to 324 nM. A further heterocycle alteration from 2-pyrrolidine (**10**; K_i, σ2 = 1312 nM) to 3-pyrrolidine (**30**; K_i, σ2 = 685 nM) resulted in a 2-fold improvement for the σ2 receptor binding, accompanied with approximately 45-fold decrease in σ1 affinity. In addition, the σ1 binding assay for compounds **10**, **13-28** and **30** showed that the introduction of substituents on the benzene ring is generally tolerated, with the exception of **28** (K_i, σ1 = 0.72 nM) being 6-fold more potent than the parent compound **10** and the methoxy-substituted **19** (K_i, σ1 = 210 nM) being the least potent σ1 binder in this series, suggesting the unfavorable effect of monosubstitution with an EDG.

Table 1. The σ2 receptor binding profiles for analogues **10**, **13-28**, and **30**.

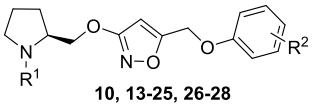

10, 13-25, 26-28

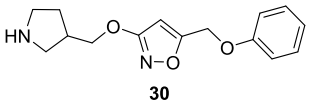

30

Analogue	R^1	R^2	K_i σ1[a] (nM)	K_i σ2[a] (nM)
10[b]	H	H	4.1 ± 0.7	1312[c]
13	H	2-F	6.0 ± 0.8	396 ± 72
14	H	3-F	1.4 ± 0.2	277 ± 32
15	H	4-F	4.4 ± 0.6	471 ± 54

16	H	3-CF_3	6.6 ±0.6	88 ±12
17	H	4-CF_3	13.3 ±1.2	91.7 ±10
18	H	4-Cl	13.0 ±1.5	139 ±16
19	H	4-OCH_3	210 ±19	675 ±138
20	H	3-F, 4-F	4.71 ±0.54	373 ±44
21	H	3-Cl, 4-Cl	12.1 ±1.4	46.5 ±8.5
22	H	3-Cl, 5-Cl	4.59 ±0.42	52.2 ±9.6
23	H	3-F, 4-Cl	10.8 ±1.0	129 ±29
24	H	3-Cl, 4-F	3.93 ±0.54	205 ±47
25	H	3-Cl, 5-F	2.78 ±0.38	258 ±58
26	CH_3	3-F, 4-Cl	3.34 ±0.54	258 ±58
27	CH_3	3-Cl, 4-F	3.73 ±0.34	324 ±74
28	CH_3	3-Cl, 5-F	0.72 ±0.10	71.3 ±7.8
30	-	-	184 ±34	685 ±109

[a]See experimental section. Radioligands: σ1, [^{3}H]-(+)-pentazocine; σ2, [^{3}H] DTG (ditolylguanidine). Receptor material: σ1, Guinea pig brain homogenate; σ2, PC12 cells. [b]The K_i values for compounds **10** and **13-19** were cited from the literature.[28-29]. [c]Data shown as average of K_i values from two measurements: 665 ±29 nM and 1958 ±392 nM.

Subsequent SAR studies were focused on the effects of: i) replacing the 2-pyrrolidine ring of compound **10** with *N*-cycloalkylaminoethoxy derivatives to probe the steric bulk at the *N*-terminal site (**35-40**; Table 2) and ii) extension of aminoalkyl groups to the *N*-terminal atom (**42**, **43**, **48-51**;

Table 2), which has proven beneficial for the σ2 receptor binding affinities in other reported scaffolds [23, 24]. The *N*-cyclopentyl derivative **36** had similar σ1 and σ2 receptor affinities with the *N*-cyclobutyl parent compound **35** [30], while the *N*-cyclohexyl analogue **37** showed an improvement for σ2 receptor affinity with a K_i value of 23 nM, which is a 9-fold increase relative to the *N*-cyclobutyl analogue **35**. However, the affinity of compound **37** for σ1 decreased by an order of magnitude compared to the ring-contracted analogs, indicating that at this *N*-terminal site, the larger steric hindrance confers a preference for σ2 receptor affinity over the σ1. Keeping the cyclohexyl substituent intact, further substitution at the benzene ring region was introduced, such as *m*, *p*-dichloro (**38**) and *m*-trifluoromethyl (**39**), to give single digit nanomolar σ2 receptor ligands with K_i values of 1.8 nM and 2.5 nM, respectively. As seen in compounds **23-28**, *N*-methylation of compound **39** resulted in compound **40** (K_i = 4.4 nM) which maintained the binding affinity at σ2 receptor. However, concurrent introduction of *N*-methyl and dimethylamide group at the cyclohexyl ring (**42**) resulted in a significant reduction for σ2 affinity (K_i = 1008 nM). Reduction of the dimethylamide compound **42** resulted in the dimethylamino analogue **43** with K_i value of 76.6 nM at the σ2 receptor. In order to examine further effects of aminoalkyl substituents around the *N*-terminal region, installation of aminoalkyl groups with varying length to the original 2-pyrrolidine group (**48-51** vs **10**) resulted in highly potent σ2 receptor ligands with binding affinities ranging from 7.9 nM to 74.7 nM. Compound **48** (K_i = 74.7 nM) with 6C-aminoalkyl substitution had 18-fold increase on σ2 affinity when compared to the parent compound **10**. Introduction of a 3-trifluoromethyl group (**48** vs **49**) on the phenolic ether region resulted in compound **49** with a K_i (σ2) value of 8.5 nM. The 3,4-dichlorosubstituted analogue **50** displayed a very similar σ2 affinity to compound **49** (K_i = 10.3 nM) and chain contraction from a 6C to 4C (compound **51**; K_i = 7.9 nM) was tolerated. In summary,

although introduction of methyl groups to the nitrogen atom may not be conducive for σ2 receptor affinity, incorporation of the alkyl amino groups (**48-51**) proved to be beneficial for optimal σ2 binding.

Table 2. σ2 receptor binding profiles for analogues **35-40**, **42, 43,** and **48-51.**

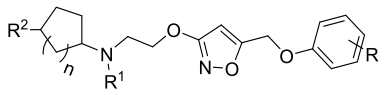

35-40, 42, 43

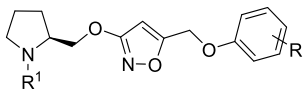

48-51

Analogue	R^1	R^2	n	R	K_i σ1[a] (nM)	K_i σ2[a] (nM)
35[b]	H	H	0	H	0.2 ± 0.0	198 ± 64
36	H	H	1	H	0.48 ± 0.044	268 ± 48
37	H	H	2	H	2.83 ± 0.26	22.8 ± 4.2
38	H	H	2	3-Cl, 4-Cl	NT[c]	1.81 ± 0.33
39	H	H	2	3-CF_3	NT	2.53 ± 0.35
40	CH_3	H	2	3-CF_3	NT	4.44 ± 0.81
42	CH_3	-$CON(CH_3)_2$	2	H	NT	1008 ± 138
43	CH_3	-$CH_2N(CH_3)_2$	2	H	NT	76.6 ± 10
48	-$(CH_2)_6NH_2$	-	-	H	/[d]	74.7 ± 8.6
49	-$(CH_2)_6NH_2$	-	-	3-CF_3	/	8.46 ± 1.5
50	-$(CH_2)_6NH_2$	-	-	3-Cl, 4-Cl	/	10.3 ± 1.4
51	-$(CH_2)_4NH_2$	-	-	3-Cl, 4-Cl	/	7.92 ± 1.1

[a] See experimental section. Radioligands: σ1, [^{3}H]-(+)-pentazocine; σ2, [^{3}H] DTG (ditolylguanidine). Receptor material: σ1, Guinea pig brain homogenate; σ2, PC12 cells. [b] The K_i value for compound

35 are cited from the literature. [30] [c] not tested; [d] See supporting information Table S1.

In order to obtain a preliminary binding data of the newly synthesized analogues on the σ1 receptor, selected compounds **16, 21, 30, 36, 37, 48-51** were tested at a single concentration on guinea pig σ1 receptor. The percentage inhibition data of compounds at 10 μM against [^{3}H]-(+)-pentazocine are listed in Supporting Information Table S1. Compounds **16, 21, 36,** and **37** were identified to be the most potent σ1 binders with 93-97% inhibitory activities, correlating to the observed K_i values of 0.48 to 12.1 nM. On the other hand, compound **30** had 85.9% inhibition on the guinea pig σ1 assay, corresponding to an observed K_i value of 184 nM. Compounds **48-51** all had 16.1-77.8% inhibition on the guinea pig σ1 assay, indicative of triple digit nanomolar K_i values, although further experiments are still needed. In order to further obtain a rough predictive correlation for these preliminary σ1 binding results, we conducted molecular docking studies on compounds **21** (K_i, σ1 = 12.1 ± 1.4 nM – this value obtained from Psychoactive Drug Screening Program) and **51** (% inhibition of 77.8% at the guinea pig σ1 receptor) utilizing the solved crystal structure of σ1 (PDB ID 5HK1). The protein structure was prepared by Protein Preparation Wizard, and missing atoms and all hydrogen atoms were added to the protein according to their local environment in the step. All compounds were flexibly docked into the binding pocket defined by residues W89, M93, L95, Y103, L105, F107, I124, D126, W164, and E172 using Glide with XP scoring function. Most reasonable poses were selected for visualization analysis. The σ1 interactions with each compound were pictured using Pymol. All of the molecular docking work was performed using the Maestro software. The proposed binding modes are shown in Figure S2, demonstrating the formation of hydrogen bond between Y103, E172 and basic nitrogen atom of the pyrrolidine (compound **21**; Figure S2A; Glide

score of -9.0) which is crucial for σ1 receptor binding affinity, consistent with a reported literature [8]. On the other hand, introduction of an aminoalkyl group on the pyrrolidine nitrogen (compound **51**; Glide score of -6.1) resulted in its retroflexed conformation in the receptor pocket and therefore no longer capable of forming an effective H-bond, consistent with the weak σ1 affinity (Figure S2B).

Evaluation of Alkoxyisoxazole-based σ2 Receptor Ligands against Osteosarcoma Cells

Although the role of σ2 receptor has been implicated in various tumor progression, thus far there have been very limited number of reports with respect to its role in osteosarcoma. Osteosarcoma is the most common bone tumor and one of the most harmful tumors, which often occurs in young children and the elderly [31]. Although the 5-year survival rate of osteosarcoma is 60%, it is highly prone to metastasis, including primary and secondary metastasis [31c, 32]. Once metastasis of osteosarcoma occurs, its 5-year survival rate drops to 19% [32b, 33], while the survival rates of pulmonary metastasis and bone metastases were 23% and 0% respectively [31c]. The pathogenesis of osteosarcoma is complex and remains to be well understood, with some studies demonstrating the role of mutations in the retinoblastoma gene and p53 proteins [34]. To date, there is still no ideal therapeutic for osteosarcoma, which is generally treated with two or more anticancer drugs in combination, including doxorubicin, methotrexate, and cisplatin [35]. With these considerations in mind, selected alkoxyisoxazoles analogues with potent σ2 receptor affinities (compounds **21, 37, 38-40**, **49-51**) along with compound **10** were tested for their antiproliferative activities against the human osteosarcoma cell 143B (Table 3). The *N*-aminoalkyl chain compounds **49-51** displayed respectable antiproliferative activities with IC_{50} values ranging from 0.89-2.81 μM while the other tested compounds were not active (IC_{50} > 10 μM). Siramesine was included as a positive control in

this assay and found to also be effective with an IC_{50} value of 1.81 μM. Although it remains to be seen whether or not inhibition of both σ1 and σ2 receptors are required, it is clear for the alkoxylisoxazole scaffold that the *N*-aminoalkyl chain extension from the pyrrolidine ring represents an important structural element for the observed antiproliferative activity in osteosarcoma cells.

Table 3. Antiproliferative activities of selected compounds against osteosarcoma cell line 143B.

Compound	K_i σ2 (nM)[a]	IC_{50} (μM)[b]
10	1312	> 10
21	46.5 ± 8.5	> 10
37	22.8 ± 4.2	> 10
38	1.81 ± 0.33	> 10
39	2.53 ± 0.35	> 10
40	4.44 ± 0.81	> 10
49	8.46 ± 1.5	2.81 ± 0.12
50	10.3 ± 1.4	3.02 ± 0.12
51	8.02 ± 1.1	0.89 ± 0.02
Siramesine	0.12	1.81 ± 0.05

[a] See experimental section. Radioligands: σ2, [^{3}H] DTG (ditolylguanidine); The K_i values listed in this table are the average ± SEM from a minimum of 3 saturation binding assays. [b] Osteosarcoma cell lines were treated with σ2 ligands (gradient concentration) or DMSO vehicle for 48 h, and cell viability relative to vehicle was determined by crystal violet assay method (Mean ± SEM, n ≥ 3).

Cytotoxicity against Osteosarcoma Cells and Normal Cells

As a preclinical experimental antitumor drug, siramesine is widely regarded as the compound of choice for comparison studies in the evaluation of novel σ2 receptor ligands against various tumors [19e, 19i, 23b]. Cytotoxic activities of the ligands against two osteosarcoma cell lines 143B and MOS-J (Figure 2A and 2B) were expressed as concentration-dependent inhibition curves. The results showed that the inhibitory effect of alkoxyisoxazole **51** on the proliferation of both osteosarcoma cell lines was significantly stronger than that of the positive control siramesine with IC_{50} values of 0.89 and 0.71 μM vs. 1.81 and 2.01 μM for 143B and MOS-J cells respectively. As seen in Figure 2C, compound **51** also displayed reduced cytotoxicity to the tested normal cells, including human immortalized keratinocytes HaCaT (IC_{50} = 6.47 μM), human embryonic villous cells HAF (IC_{50} = 3.35 μM) and human normal embryonic liver cells LO2 (IC_{50} > 10 μM).

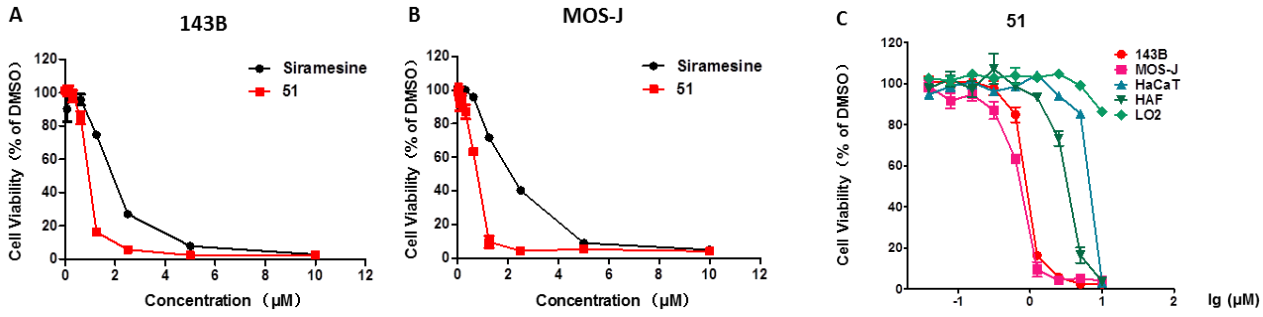

Figure 2. A-B. Effects of **51** and siramesine on cell viability was concentration-dependent in different osteosarcoma cell lines. After seeding for 12 h, 143B and MOS-J cells were treated in the presence of DMSO vehicle or indicated concentrations of **51** and siramesine. Cells were incubated for 48 h and cell viability relative to vehicle was determined by crystal violet assay method ($n \geq 3$; bars, SEM); C. Osteosarcoma cells (143B and MOS-J) and normal cells (HaCaT, HAF, and LO2) were treated in the presence of DMSO vehicle or different concentrations of the σ2 ligands for 48 h.

Then cell viability relative to vehicle was determined by crystal violet assay method (n ≥ 3; bars, SEM).

Inhibition of the Colony Formation Ability of Osteosarcoma Cells

To further gain insights into the antiproliferative activity, the abilities of the alkoxyisoxazole-based σ2 ligands to inhibit colony formation was assessed [36]. The clonogenic assay is principally a measure of the cell abilities to undergo unlimited division and often used as an assay of choice for determining the effectiveness of cytotoxic agents. As can be seen in Figure 3, head-to-head comparison of compound **51** vs siramesine was conducted at 1 and 2 μM concentrations. The number of cells forming colony under co-cultivation with siramesine and compound **51** were significantly reduced compared to the DMSO control group suggesting that both **51** and siramesine were able to suppress long-term clonogenic survival and trigger apoptosis.

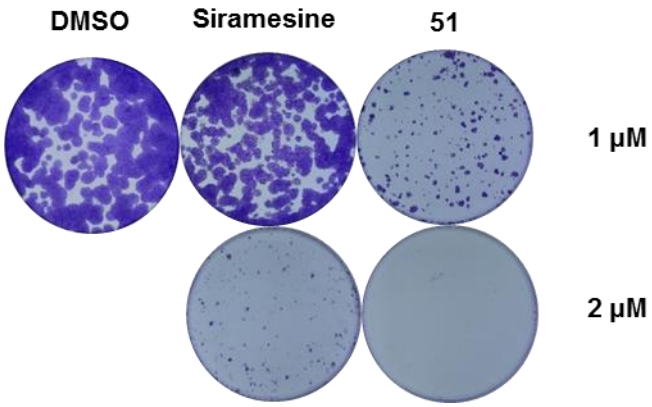

Figure 3. σ2 ligands inhibited the colony-formation ability of osteosarcoma cell. 143B cells were plated at a density of 1000 cells per well in six-well plates. After 24 h of adhesion, cells were treated with compound **51** or DMSO at appropriate density for the experimental goals, and fixed after culture for another 10 days.

Apoptosis and Cell Cycle Analysis of 3-Alkoxyisoxazole 51 against Osteosarcoma Cells

Cell cycle analysis was performed in the osteosarcoma cell line (Figure 4A,B) as there have been reports that σ2 receptor ligands may impair the cell cycle [23b]. When compared to the vehicle control group whereby the proportion of cells was 47.5%, 40.6%, and 11.9% in the G_0G_1 phase, S phase and G_2M phase respectively, the experimental group treated with compound **51** showed the proportion of cells being 56.6%, 37.8%, and 5.6% in the G_0G_1 phase, S phase and G_2M phase respectively. These results suggest that compound **51** could induce cell-cycle arrest in the G_0G_1 phase. Furthermore, some σ2 receptor ligands are reported in the literature to inhibit tumor growth in various animal models by promoting apoptosis [18, 19c, 23]. Within this context, the osteosarcoma cells 143B was treated with compound **51** in order to confirm the ability of this compound to induce apoptosis (Figure 4C). Through fluorescence activated cell sorting (FACS) analysis of apoptosis by Annexin V assay, up to 33.4% osteosarcoma cells were in the process of apoptosis (Q2 and Q3) upon treatment with 5 μM of compound **51**. In comparison, less than 10% of the osteosarcoma cells were in the process of apoptosis in the vehicle control group. These results demonstrated that the σ2 receptor ligand **51** could inhibit the osteosarcoma cell growth by inducing apoptosis. Taken together, the observed antiproliferative activity of compound **51** in osteosarcoma cells could be mediated in part via disruption of the cell cycle and induction of cell apoptosis.

10.1002/cmdc.202000461

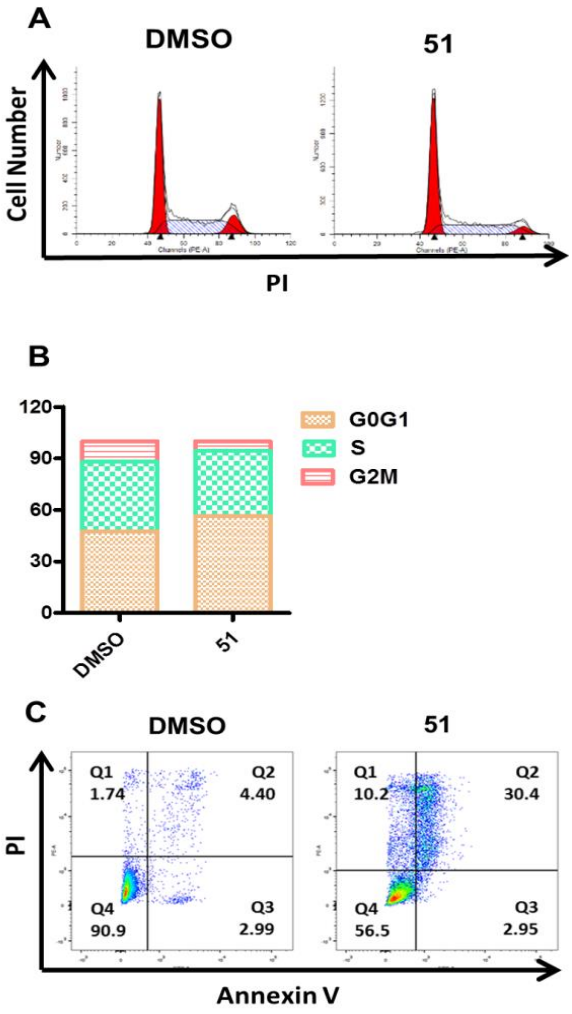

Figure 4. Apoptosis and cell cycle analysis with 143B cells grown in 10% FBS complete medium. (A, B) Effect of compound **51** (5 μM) on cell cycle of 143B cells. Cells were treated with ligand for 24 h, then harvested, fixed in ethanol (80%) and stained with propidium iodide. Results were expressed as percentage of cells residing in different phase of cell cycle. (C) FACS analysis of apoptosis by Annexin V assay. Cells were exposed for 12 h to compound **51** (5 μM). Q1 area represents necrotic cells; Q2 late-apoptotic cells; Q3 early-apoptotic cells; Q4 viable cells. The images are representative of three experiments.

Conclusions

This present study represents a continuation of our SAR work on the 3-alkoxyisoxazole scaffold as a versatile ligands for σ receptors. Various EWGs are tolerated in the phenolic ether region (compounds **13**-**30**; Table 1), however these compounds are mostly potent at the σ1 receptor. In this work, replacement of the 2-pyrrolidine ring with the *N*-cycloalkylaminoethoxy derivatives (**35**-**40**, **42**, **43**; Table 2) and further extension of aminoalkyl chains to the pyrrolidine nitrogen atom (**48**-**51**; Table 2) resulted in a number of 3-alkoxyisoxazoles derivatives with potent σ2 receptor binding affinities, i.e. those with K_i values of less than 100 nM (compounds **21**, **22**, **28**, **37**-**40**, **43**, **48**-**51**). Evaluation of selected most potent σ2 ligands to inhibit the proliferation of osteosarcoma cells identified compound **51** (K_i σ2 = 7.9 nM) as the most active analogue, with IC_{50} values of 0.89 μM and 0.71 μM on 143B and MOS-J cells, respectively. Furthermore, compound **51** was demonstrated to inhibit clone formation, induce cell-cycle arrest and apoptosis of osteosarcoma cells. While it remains to be seen whether or not inhibition of both σ1 and σ2 receptors are necessary for antiproliferative activity of the alkoxyisoxazoles in osteosarcoma cells, it is clear that the extra aminoalkyl chain on the pyrrolidine ring is needed. Overall, this study represents the potential use of 3-alkoxyisoxazole-based σ2 receptor ligand **51** for the treatment of osteosarcoma. In vivo studies on osteosarcoma mice models will be performed in the near future.

Experimental section

Chemistry

General methods

All starting reagents and solvents were obtained commercially and used without further purification,

except that anhydrous THF and CH_2Cl_2 were acquired by distillation over sodium or CaH_2, respectively. All non-aqueous reactions were run under an inert atmosphere without moisture. The progress of reactions was monitored by TLC performed on silica gel GF254 or dipping into $KMnO_4$ solution or phosphomolybdic acid solution followed by heating. Silica gel for column chromatography (CC) was of 200−300 mesh particle size. ^1H and ^{13}C NMR spectra were recorded on a Bruker Advance III 400 spectrometer at 400 MHz (^1H) and 101 MHz (^{13}C). Specific rotation was performed on Rudolph Research Analytical Autopol VI Polarimeter (λ = 589 nm, T = 20 ºC). High resolution mass spectra were performed using a Bruker ESI-TOF high-resolution mass spectrometer. Purity of all final compounds (> 95%) was detected by analytical HPLC, which was carried out on an Agilent 1200 HPLC system with a ZORBAX Eclipse XDB-C18 column, with detection at 220, 254, or 270 nm on a variable wavelength detector G1365D; flow rate = 1.4 mL/min; gradient of 0−100% methanol in water (both containing 0.05 vol% of TFA) in 25 min.

General procedures

The procedure for *N-tert*-butoxycarbonyl protection reaction (A). To a stirred suspension of amine (6.0 mmol) and K_2CO_3 (12 mmol) in THF/H_2O (20 mL, 1:1) was added di-*tert* butyl bicarbonate (6.3 mmol) slowly at 0 ℃ under the nitrogen. After stirring 3h at rt, the suspension was diluted with water (50 mL) and extracted by EtOAc (30 mL × 3), the combined organic layer was washed by brine, dried over Na_2SO_4 and evaporated in *vacuo*. The residue was purified by flash chromatography to give the product.

The procedure for the preparation of iodide (B). To a stirred solution of alcohol (1.4 mmol), imidazole (4.2 mmol), and PPh_3 (2.1 mmol) in anhydrous CH_2Cl_2 (20 mL) was added I_2 (2.1 mmol) with ice cooling under nitrogen. After stirring 2h at rt, the solvent was evaporated and the residue

was purified by flash chromatography to give the iodide product.

The procedure for the preparation of phenyl ethers (C). To a stirred solution of an iodide (0.9 mmol) and substituted phenol (1.8 mmol) in anhydrous DMF (4 mL) was added K_2CO_3 (2.7 mmol) under N_2. After stirring overnight at rt, the mixture was diluted with water (50 mL) and extracted with EtOAc (2×30 mL), then the combined organic layer were washed with brine (30 mL), dried over Na_2SO_4, concentrated in vacuum and the residue was purified by flash chromatography to give the product and advanced to the next step without further purification.

The procedure for *N*-*tert*-butoxycarbonyl deprotection reaction (D). D1： To a solution of the *N*-Boc protected compound (0.39 mmol) in EtOAc (2 mL) was added HCl/EtOAc (2 mol/L, 2 mL) under nitrogen. After stirring overnight, the solvent was evaporated and the residue was triturated with diethyl ether (10 mL). The precipitate was filtered to give the HCl salt. **D2：** To a solution of the *N*-Boc protected compound (0.39 mmol) in CH_2Cl_2 (10 mL) was added TFA (1 mL). After stirring overnight the solvent was removed and the residue was purified by preparation HPLC followed by lyophilized to obtain the TFA salt.

The procedure for *N*-methylation reaction (E). To a solution of amine (1.0 mmol) and HCHO (1.0 mL) in CF_3CH_2OH (4 mL) was added $NaBH_4$ (1.2 mmol) at 0 ℃ under nitrogen. After stirring for 2 h at 40 ℃, the solvent was diluted with EtOAc (40 mL), washed with water (40 mL) and brine (30 mL), dried over Na_2SO_4 and concentrated under vacuum. The residue was purified by flash chromatography to give *N*-methylation product**.**

The procedure for *N*-cycloalkylation reaction (F). To a solution of amine (1.0 mmol), ketone (1.2 mmol) and acetic acid (0.1 mL) in CH_3OH (20 mL) was added $Na(CN)BH_3$ (1.4 mmol) at rt under nitrogen. After stirring overnight, the solvent was diluted with EtOAc (40 mL), washed with water

(40 mL) and brine (30 mL), dried over Na_2SO_4 and concentrated under vacuum. The residue was purified by flash chromatography to give *N*-cycloalkylation product.

The procedure for *N*-aminoalkylation reaction (G). A solution of reactant (0.55 mmol) and iodide (0.77 mmol) dissolved in anhydrous DMF (4 mL) was added K_2CO_3 (2.2 mmol) under N_2. After stirring for 12 h at rt, the mixture was diluted with water (50 mL) and extracted with EtOAc (3×30 mL), then the combined organic layers were washed with water (80×2 mL) and brine (50 mL), dried over Na_2SO_4, concentrated in *vacuo* and the residue was purified by flash chromatography to give the product.

***(S)*-2-(((5-((2-Fluorophenoxy)methyl)isoxazol-3-yl)oxy)methyl)pyrrolidin-1-ium chloride (13).** This compound was obtained from **12** and 2-fluorophenol employing methods C and D1. White solid; total yield 55% for 2 steps; purity 98.0%; $[\alpha]_D^{20}$ = + 13 (*c* = 1 mg/mL, MeOH). ^{1}H NMR (400 MHz, DMSO-d_6) δ 9.90 (br s, 1H), 9.39 (br s, 1H), 7.37–7.19 (m, 2H, phenol), 7.18–7.11 (m, 1H, phenol), 7.00 (s, 1H, phenol), 6.47 (s, 1H, isoxazol), 5.27 (s, 2H, CH_2-O-phenol), 4.44–4.38 (m, 2H, CH_2-O-isoxazol), 3.91–3.87 (m, 1H, pyrrolidin), 3.18–3.16 (m, 2H, pyrrolidin), 2.22–1.99 (m, 1H, pyrrolidin), 1.97–1.78 (m, 2H, pyrrolidin), 1.73–1.54 (m, 1H, pyrrolidin). ^{13}C NMR (101 MHz, DMSO-d_6) δ 170.7 (isoxazol), 168.5 (isoxazol), 151.7 (d, $J_{C\text{-}F}$ = 247.0 Hz, phenol), 145.2 (d, $J_{C\text{-}F}$ = 10.3 Hz, phenol), 124.8 (d, $J_{C\text{-}F}$ = 3.4 Hz, phenol), 122.2 (d, $J_{C\text{-}F}$ = 6.9 Hz, phenol), 116.2 (d, $J_{C\text{-}F}$ = 18.3 Hz, phenol), 115.6 (phenol), 95.8 (isoxazol), 68.4 (C-O-phenol), 61.3 (C-O-isoxazol), 57.3 (pyrrolidin), 44.9 (pyrrolidin), 26.1(pyrrolidin) , 23.2 (pyrrolidin). HRMS (ESI): calcd for $C_{15}H_{18}FN_2O_3$ $[M+H]^+$, 293.1296; found, 293.1293. The interpretation of ^{1}H and ^{13}C NMR signals of **14**-**30** are similar with **13**.

***(S)*-2-(((5-((3-Fluorophenoxy)methyl)isoxazol-3-yl)oxy)methyl)pyrrolidin-1-ium chloride (14).**

This compound was obtained from **12** and 3-fluorophenol employing methods C and D1. White solid; total yield 51% for 2 steps; purity 97.9%; $[\alpha]_D^{20}$ = + 9.3 (*c* = 1 mg/mL, MeOH). ^{1}H NMR (400 MHz, DMSO-d_6) δ 9.29 (br s, 2H), 7.35 (q, *J* = 8.3 Hz, 1H), 6.95 (dt, *J* = 11.2, 2.4 Hz, 1H), 6.89 (dd, *J* = 8.3, 2.4 Hz, 1H), 6.83 (td, *J* = 8.6, 2.4 Hz, 1H), 6.47 (s, 1H), 5.23 (s, 2H), 4.44 (dd, *J* = 11.2, 3.9 Hz, 1H), 4.36 (dd, *J* = 11.2, 8.2 Hz, 1H), 3.91 (qd, *J* = 8.1, 3.8 Hz, 1H), 3.25–3.12 (m, 2H), 2.16–2.05 (m, 1H), 2.01–1.83 (m, 2H), 1.77–1.65 (m, 1H). ^{13}C NMR (101 MHz, DMSO-d_6) δ 170.8, 168.6, 162.9 (d, $J_{C\text{-}F}$ = 244.1 Hz), 158.8 (d, $J_{C\text{-}F}$ = 11.1 Hz), 130.8 (d, $J_{C\text{-}F}$ = 10.1 Hz), 111.1, 108.1 (d, $J_{C\text{-}F}$ = 21.3 Hz), 102.4 (d, $J_{C\text{-}F}$ = 25.4 Hz), 95.7, 68.4, 60.8, 57.3, 44.9, 26.2, 23.2. HRMS (ESI): calcd for $C_{15}H_{18}FN_2O_3$ $[M+H]^+$, 293.1296; found, 293.1293.

***(S)*-2-(((5-((4-Fluorophenoxy)methyl)isoxazol-3-yl)oxy)methyl)pyrrolidin-1-ium chloride (15).** This compound was obtained from **12** and 4-fluorophenol employing methods C and D1. White solid; total yield 53% for 2 steps; purity 96.1%, $[\alpha]_D^{20}$ = + 11 (*c* = 1 mg/mL, MeOH). ^{1}H NMR (400 MHz, DMSO-d_6) δ 9.77 (br s, 1H), 9.26 (br s, 1H), 7.19–7.11 (m, 2H), 7.10–7.02 (m, 2H), 6.44 (s, 1H), 5.18 (s, 2H), 4.49–4.33 (m, 2H), 3.97–3.83 (m, 1H), 3.25–3.12 (m, 2H), 2.15–2.04 (m, 1H), 2.01–1.81 (m, 2H), 1.74–1.65 (m, 1H). ^{13}C NMR (101 MHz, DMSO-d_6) δ 170.8, 169.1, 157.0 (d, $J_{C\text{-}F}$ = 237.8 Hz), 153.7 (d, $J_{C\text{-}F}$ = 1.9 Hz), 116.3 (d, $J_{C\text{-}F}$ = 8.2 Hz), 116.0 (d, $J_{C\text{-}F}$ = 23.2 Hz), 95.6, 68.5, 61.1, 57.4, 45.1, 26.2, 23.3. HRMS (ESI): calcd for $C_{15}H_{18}FN_2O_3$ $[M+H]^+$, 293.1296; found, 293.1293.

***(S)*-2-(((5-((3-(Trifluoromethyl)methyl)isoxazol-3-yl)oxy)methyl)pyrrolidin-1-ium-2,2,2-trifluor oacetate (16).** This compound was obtained from **12** and 3-trifluoromethylphenol employing method C and D2. Yellow oil; total yield 34% for 2 steps; purity 98.5%; $[\alpha]_D^{20}$ = + 22 (*c* = 1 mg/mL, MeOH). ^{1}H NMR (400 MHz, DMSO-d_6) δ 9.59 (br s, 1H), 9.06 (br s, 1H), 7.56 (t, *J* = 8.0 Hz, 1H), 7.37 (m, 2H), 6.47 (s, 1H), 5.32 (s, 2H), 4.45 (dd, *J* = 8.0, 4.0 Hz, 1H), 4.34 (dd, *J* = 10.0, 4.0 Hz, 1H), 3.96

(m, 1H), 3.23 (t, J = 6.0 Hz, 2H), 2.18-2.06 (m, 1H), 2.04–1.81 (m, 2H), 1.81–1.61 (m, 1H). ^{13}C NMR (101 MHz, DMSO-d_6) δ 170.8, 168.6, 158.5 (TFA), 157.7, 130.8, 130.2 (q, $J_{C–F}$ = 31.6 Hz), 123.8 (q, $J_{C–F}$ = 271.0 Hz), 119.0, 118.0 (q, $J_{C–F}$ = 4.0 Hz), 115.6 (TFA), 111.4 (q, $J_{C–F}$ = 4.0 Hz), 95.6, 68.4, 60.8, 57.5, 45.2, 26.0, 23.3. HRMS (ESI): calcd for $C_{16}H_{18}F_3N_2O_3$ $[M+H]^+$, 343.1264; found, 343.1281.

***(S)*-2-(((5-((4-(Trifluoromethyl)phenoxy)methyl)isoxazol-3-yl)oxy)methyl) pyrrolidin-1-ium chloride (17).** This compound was obtained from **12** and 4-trifluoromethylphenol employing methods C and D1. White solid; total yield 36% for 2 steps; purity 98.1%; $[\alpha]_D^{20}$ = + 17 (c = 1 mg/mL, MeOH). ^{1}H NMR (400 MHz, DMSO-d_6) δ 9.40 (br s, 1H), 8.96 (br s, 1H), 7.69 (d, J = 8.6 Hz, 2H), 7.23 (d, J = 8.6 Hz, 2H), 6.48 (s, 1H), 5.32 (s, 2H), 4.45 (dd, J = 11.2, 3.6 Hz, 1H), 4.40–4.27 (m, 1H), 3.94 (dd, J = 7.9, 3.3 Hz, 1H), 3.22 (t, J = 6.6 Hz, 2H), 2.19–2.04 (m, 1H), 2.04–1.84 (m, 2H), 1.80-1.64 (m, 1H). ^{13}C NMR (101 MHz, DMSO-d_6) δ 170.8, 168.6, 160.2, 127.04 (q, J_{C-F} = 3.7 Hz), 124.4 (q, J_{C-F} = 271.9 Hz), 122.0 (q, J_{C-F} = 32.2 Hz), 115.3, 95.7, 68.5, 60.7, 57.6, 45.3, 26.0, 23.3. HRMS (ESI): calcd for $C_{16}H_{18}F_3N_2O_3$ $[M+H]^+$, 343.1264; found, 343.1296.

***(S)*-2-(((5-((4-Chlorophenoxy)methyl)isoxazol-3-yl)oxy)methyl)pyrrolidin-1-ium-2,2,2-trifluoro acetate (18).** This compound was obtained from **12** and 4-chlorophenol employing methods C and D2. White solid; total yield 46% for 2 steps; purity 97.1%; $[\alpha]_D^{20}$ = + 8.3 (c = 1 mg/mL, MeOH). ^{1}H NMR (400 MHz, DMSO-d_6) δ 9.44 (br s, 1H), 8.93 (br s, 1H), 7.36 (d, J = 9.0 Hz, 2H), 7.07 (d, J = 8.9 Hz, 2H), 6.44 (s, 1H), 5.21 (s, 2H), 4.44 (dd, J = 11.2, 3.6 Hz, 1H), 4.33 (dd, J = 11.0, 8.6 Hz, 1H), 3.94 (s, 1H), 3.21–3.17 (m, 2H), 2.17-2.06 (m, 1H), 2.02-1.84 (m, 2H), 1.77–1.64 (m, 1H). ^{13}C NMR (101 MHz, DMSO-d_6) δ 170.8, 168.9, 158.1 (TFA), 156.2, 129.3, 125.2, 116.9 (TFA), 116.6, 95.5, 68.5, 60.8, 57.6, 45.3, 26.0, 23.3. HRMS (ESI): calcd for $C_{15}H_{18}ClN_2O_3$ $[M+H]^+$, 309.1000;

found, 309.0996.

***(S)*-2-(((5-((4-Methoxyphenoxy)methyl)isoxazol-3-yl)oxy)methyl)pyrolidin-1-ium-2,2,2-trifluoro acetate (19).** This compound was obtained from **12** and 4-methoxyphenol employing methods C and D2. White solid; total yield 57% for 2 steps; purity 98.9%; $[\alpha]_D^{20}$ = + 16 (*c* = 1 mg/mL, MeOH). ^{1}H NMR (400 MHz, DMSO-d_6) δ 9.40 (br s, 1H), 8.94 (br s, 1H), 6.97 (d, *J* = 9.0 Hz, 2H), 6.87 (d, *J* = 9.0 Hz, 2H), 6.41 (s, 1H), 5.12 (s, 2H), 4.44 (dd, *J* = 11.2, 3.5 Hz, 1H), 4.36–4.24 (m, 1H), 3.94 (d, *J* = 7.7 Hz, 1H), 3.70 (s, 3H), 3.21 (t, *J* = 6.8 Hz, 2H), 2.22–2.01 (m, 1H), 2.03–1.77 (m, 2H), 1.81–1.58 (m, 1H). ^{13}C NMR (101 MHz, DMSO-d_6) δ 170.7, 169.5, 157.1 (TFA), 153.9, 151.3, 117.2 (TFA), 115.8, 114.6, 95.2, 68.5, 61.1, 57.6, 55.3, 45.3, 26.0, 23.3. HRMS (ESI): calcd for $C_{16}H_{21}N_2O_4$ $[M+H]^+$, 305.1496; found, 305.1517.

***(S)*-2-(((5-((3,4-Difluorophenoxy)methyl)isoxazol-3-yl)oxy)methyl)pyrro-ledin-1-ium chloride (20).** This compound was obtained from **12** and 3,4-difluorophenol employing methods C and D1. White solid; total yield 30% for 2 steps; purity 98.9%; $[\alpha]_D^{20}$ = + 17 (*c* = 1 mg/mL, MeOH). ^{1}H NMR (400 MHz, D_2O) δ 7.13 (q, *J* = 9.9 Hz, 1H), 6.91–6.86 (m, 1H), 6.78–6.67 (m, 1H), 6.21 (s, 1H), 5.06 (s, 2H), 4.48 (dd, *J* = 11.5, 3.2 Hz, 1H), 4.31 (dd, *J* = 11.4, 7.8 Hz, 1H), 4.03 (qd, *J* = 8.1, 3.3 Hz, 1H), 3.33 (t, *J* = 7.2 Hz, 2H), 2.25–2.12 (m, 1H), 2.13–1.92 (m, 2H), 1.88–1.78 (m, 1H). ^{13}C NMR (101 MHz, D_2O) δ 171.2, 169.1, 153.4 (dd, $J_{C\text{-}F}$ = 9.0, 2.3 Hz), 151.0 (dd, $J_{C\text{-}F}$ = 247.7, 13.9 Hz), 145.5 (dd, $J_{C\text{-}F}$ = 239.8, 12.7 Hz), 117.0 (dd, $J_{C\text{-}F}$ = 18.8, 1.2 Hz), 111.0 (dd, $J_{C\text{-}F}$ = 6.3, 3.4 Hz), 105.0 (d, $J_{C\text{-}F}$ = 20.7 Hz), 95.5, 68.1, 62.0, 58.5, 45.9, 25.7, 23.3. HRMS (ESI): calcd for $C_{15}H_{17}F_2N_2O_3$ $[M+H]^+$, 311.1202; found, 312.1206.

***(S)*-2-(((5-((3,4-Dichlorophenoxy)methyl)isoxazol-3-yl)oxy)methyl)pyro-lidin-1-ium chloride (21).** This compound was obtained from **12** and 3,4-dichlorophenol employing methods C and D1.

White solid; total yield 38% for 2 steps; purity 97.0%; $[\alpha]_D^{20}$ = + 13 (*c* = 1 mg/mL, MeOH). ^{1}H NMR (400 MHz, DMSO-d_6) δ 9.60 (br s, 2H), 7.57 (d, *J* = 8.9 Hz, 1H), 7.40 (s, 1H), 7.08 (d, *J* = 8.5 Hz, 1H), 6.48 (s, 1H), 5.27 (s, 2H), 4.42 (d, *J* = 7.4 Hz, 2H), 4.02–3.79 (m, 1H), 3.18 (d, *J* = 6.5 Hz, 2H), 2.24–2.01 (m, 1H), 2.01–1.78 (m, 2H), 1.77–1.65 (m, 1H). ^{13}C NMR (101 MHz, DMSO-d_6) δ 170.8, 168.4, 156.8, 131.7, 131.1, 123.4, 116.8, 115.8, 95.8, 68.5, 61.1, 57.3, 44.9, 26.2, 23.2. HRMS (ESI): calcd for $C_{15}H_{17}Cl_2N_2O_3$ $[M+H]^+$, 343.0611; found, 343.0631.

***(S)*-2-(((5-((3,5-Dichlorophenoxy)methyl)isoxazol-3-yl)oxy)methyl)pyro-lidin-1-ium chloride (22).** This compound was obtained from **12** and 3,5-dichlorophenol employing methods C and D1. White solid; total yield 46% for 2 steps; purity 95.3%; $[\alpha]_D^{20}$ = + 14 (*c* = 1 mg/mL, MeOH). ^{1}H NMR (400 MHz, DMSO-d_6) δ 9.61 (br s, 1H), 9.13 (br s, 1H), 7.23 (t, *J* = 1.6 Hz, 1H), 7.19 (d, *J* = 1.6 Hz, 2H), 6.48 (s, 1H), 5.29 (s, 2H), 4.50–4.30 (m, 2H), 3.98–3.85 (m, 1H), 3.24–3.11 (m, 2H), 2.14–2.05 (m, 1H), 2.00–1.84 (m, 2H), 1.77–1.65 (m, 1H). ^{13}C NMR (101 MHz, DMSO-d_6) δ 170.8, 168.3, 158.8, 134.7, 121.3, 114.3, 95.8, 68.5, 61.1, 57.4, 45.1, 26.1, 23.2. HRMS (ESI): calcd for $C_{15}H_{17}Cl_2N_2O_3$ $[M+H]^+$, 343.0611; found, 343.0608.

***(S)*-2-(((5-((4-Chloro-3-fluorophenoxy)methyl)isoxazol-3-yl)oxy)methyl) pyrrolidin-1-ium chloride (23).** This compound was obtained from **12** and 3-fluoro-4-chlorophenol employing methods C and D1. White solid; total yield 40% for 2 steps; purity 99.0%; $[\alpha]_D^{20}$ = + 17 (*c* = 1 mg/mL, MeOH). ^{1}H NMR (400 MHz, DMSO-d_6) δ 9.73 (br s, 1H), 9.23 (br s, 1H), 7.52 (t, *J* = 8.8 Hz, 1H), 7.22 (dd, *J* = 11.3, 2.8 Hz, 1H), 6.91 (dd, *J* = 8.8, 1.8 Hz, 1H), 6.48 (s, 1H), 5.25 (s, 2H), 4.59–4.22 (m, 2H), 3.91 (s, 1H), 3.20 (s, 2H), 2.20–2.04 (m, 1H), 2.01–1.83 (m, 2H), 1.77–1.61 (m, 1H). ^{13}C NMR (101 MHz, D_2O) δ 171.2, 168.8, 157.4 (d, $J_{C\text{-}F}$ = 247.1 Hz), 157.0 (d, $J_{C\text{-}F}$ = 9.9 Hz), 130.8, 113.0 (d, $J_{C\text{-}F}$ = 17.8 Hz), 111.8 (d, $J_{C\text{-}F}$ = 3.2 Hz), 104.0 (d, $J_{C\text{-}F}$ = 24.8 Hz), 95.5, 68.1, 61.6,

58.5, 45.9, 25.8, 23.3. HRMS (ESI): calcd for $C_{15}H_{17}ClFN_2O_3$ $[M+H]^+$, 327.0906; found, 327.0891.

***(S)*-2-(((5-((3-Chloro-4-fluorophenoxy)methyl)isoxazol-3-yl)oxy)methyl) pyrrolidin-1-ium chloride (24).** This compound was obtained from **12** and 3-chloro-4-fluorophenol employing methods C and D1. White solid; total yield 41% for 2 steps; purity 96.0%; $[\alpha]_D^{20}$ = + 17 (*c* = 1 mg/mL, MeOH). ^{1}H NMR (400 MHz, DMSO-d_6) δ 9.68 (br, 1H), 9.18 (br, 1H), 7.38 (t, *J* = 9.1 Hz, 1H), 7.33 (dd, *J* = 6.1, 3.1 Hz, 1H), 7.12–6.96 (m, 1H), 6.47 (s, 1H), 5.23 (s, 2H), 4.49–4.34 (m, 2H), 3.91 (s, 1H), 3.12–3.26 (m, 2H), 2.16–2.04 (m, 1H), 1.99–1.82 (m, 2H), 1.77–1.65 (m, 1H). ^{13}C NMR (101 MHz, D_2O) δ 171.2, 169.0, 153.4 (d, $J_{C\text{-}F}$ = 3.0 Hz), 153.3 (d, $J_{C\text{-}F}$ = 241.4 Hz), 120.6 (d, $J_{C\text{-}F}$ = 19.2 Hz), 117.1, 116.9, 115.1 (d, $J_{C\text{-}F}$ = 8.1 Hz), 95.5, 68.1, 62.0, 58.5, 45.9, 25.7, 23.3. HRMS (ESI): calcd for $C_{15}H_{17}ClFN_2O_3$ $[M+H]^+$, 327.0906; found, 327.0897.

***(S)*-2-(((5-((3-Chloro-5-fluorophenoxy)methyl)isoxazol-3-yl)oxy)methyl) pyrrolidin-1-ium chloride (25).** This compound was obtained from **12** and 3-chloro-4-fluorophenol employing methods C and D1. White solid; total yield 47% for 2 steps; purity 97.2%; $[\alpha]_D^{20}$ = + 17 (*c* = 1 mg/mL, MeOH). ^{1}H NMR (400 MHz, DMSO-d_6) δ 9.21 (br s, 1H), 7.10–7.03 (m, 2H), 7.03–6.97 (m, 1H), 6.47 (s, 1H), 5.28 (s, 2H), 4.50–4.40 (m, 1H), 4.40–4.30 (m, 1H), 3.92 (m, 1H), 3.20 (t, *J* = 6.8 Hz, 2H), 2.12–2.04 (m, 1H), 1.98–1.84 (m, 2H), 1.80–1.63 (m, 1H). ^{13}C NMR (101 MHz, DMSO-d_6) δ 170.8, 168.1, 162.7 (d, $J_{C\text{-}F}$ = 244.6 Hz), 159.2 (d, $J_{C\text{-}F}$ = 12.6 Hz), 134.5 (d, $J_{C\text{-}F}$ = 13.8 Hz), 111.6 (d, $J_{C\text{-}F}$ = 3.1 Hz), 109.1 (d, $J_{C\text{-}F}$ = 25.4 Hz), 101.9 (d, $J_{C\text{-}F}$ = 25.2 Hz), 95.9, 68.4, 61.1, 57.3, 44.9, 26.2, 23.2. HRMS (ESI): calcd for $C_{15}H_{17}ClFN_2O_3$ $[M+H]^+$, 327.0906; found, 327.0894.

***(S)*-5-((4-Chloro-3-fluorophenoxy)methyl)-3-((1-methylpyrrolidin-2-yl) methoxy)isoxazole (26).** This compound was obtained from **23** employing method E. Colorless oil; yield 59%; purity 95.2%; $[\alpha]_D^{20}$ = - 0.67 (*c* = 1 mg/mL, MeOH). ^{1}H NMR (400 MHz, $CDCl_3$) δ 7.09–7.02 (m, 1H), 7.01–6.94

(m, 1H), 6.83–6.74 (m, 1H), 5.98 (s, 1H), 4.99 (s, 2H), 4.29–4.15 (m, 2H), 3.14–3.05 (m, 1H), 2.65–2.55 (m, 1H), 2.43 (s, 3H), 2.30–2.23 (m, 1H), 2.04–1.91 (m, 1H), 1.84–1.68 (m, 3H). ^{13}C NMR (101 MHz, $CDCl_3$) δ 171.9, 167.8, 153.9 (d, J_{C-F} = 2.6 Hz), 153.5 (d, J_{C-F} = 243.7 Hz), 121.4 (d, J_{C-F} = 19.2 Hz), 117.0 (d, J_{C-F} = 2.9 Hz), 116.8, 114.5 (d, J_{C-F} = 6.9 Hz), 95.4, 71.7, 64.0, 62.3, 57.6, 41.4, 28.0, 22.8. HRMS (ESI): calcd for $C_{16}H_{19}ClFN_2O_3$ $[M+H]^+$, 341.1063; found, 341.1079.

***(S)*-5-((3-Chloro-4-fluorophenoxy)methyl)-3-((1-methylpyrrolidin-2-yl) methoxy)isoxazole (27).** This compound was obtained from **24** employing method E. Colorless oil; yield 45%; purity 96.3%; $[\alpha]_D^{20}$ = - 1.33 (*c* = 1 mg/mL, MeOH). ^{1}H NMR (400 MHz, $CDCl_3$) δ 7.35–7.22 (m, 1H), 6.81–6.63 (m, 2H), 5.98 (s, 1H), 5.00 (s, 2H), 4.32–4.13 (m, 2H), 3.15–3.03 (m, 1H), 2.65–2.54 (m, 1H), 2.43 (s, 3H), 2.31–2.22 (m, 1H), 2.03–1.91 (m, 1H), 1.88–1.67 (m, 3H). ^{13}C NMR (101 MHz, $CDCl_3$) δ 171.9, 167.5, 158.4 (d, J_{C-F} = 249.9 Hz), 157.3 (d, J_{C-F} = 9.6 Hz), 130.8 (d, J_{C-F} = 1.0 Hz), 113.7 (d, J_{C-F} = 18.0 Hz), 111.3 (d, J_{C-F} = 3.4 Hz), 104.1 (d, J_{C-F} = 24.5 Hz), 95.5, 71.7, 64.0, 62.0, 57.6, 41.4, 28.0, 22.8. HRMS (ESI): calcd for $C_{16}H_{19}ClFN_2O_3$ $[M+H]^+$, 341.1063; found, 341.1056.

***(S)*-5-((3-Chloro-5-fluorophenoxy)methyl)-3-((1-methylpyrrolidin-2-yl) methoxy)isoxazole (28).** This compound was obtained from **25** employing method E. Colorless oil; yield 38%; purity 98.6%; $[\alpha]_D^{20}$ = - 1.00 (*c* = 1 mg/mL, MeOH). ^{1}H NMR (400 MHz, $CDCl_3$) δ 6.78–6.73 (m, 2H), 6.58 (dt, *J* = 10.1, 2.2 Hz, 1H), 5.99 (s, 1H), 5.00 (s, 2H), 4.24 (qd, *J* = 10.5, 5.0 Hz, 2H), 3.11 (t, *J* = 8.0 Hz, 1H), 2.72–2.54 (m, 1H), 2.43 (s, 3H), 2.34–2.22 (m, 1H), 2.02–1.90 (m, 1H), 1.87–1.66 (m, 3H). ^{13}C NMR (101 MHz, $CDCl_3$) δ 171.9, 167.3, 163.3 (d, J_{C-F} = 249.9 Hz), 159.2 (d, J_{C-F} = 12.3 Hz), 135.7 (d, J_{C-F} = 13.2 Hz), 111.4 (d, J_{C-F} = 3.4 Hz), 109.9 (d, J_{C-F} = 25.1 Hz), 101.5 (d, J_{C-F} = 25.2 Hz), 95.5, 71.7, 64.0, 61.9, 57.6, 41.4, 28.0, 22.8. HRMS (ESI): calcd for $C_{16}H_{19}ClFN_2O_3$ $[M+H]^+$, 341.1063; found, 341.1066.

3-(((5-(Phenoxymethyl)isoxazol-3-yl)oxy)methyl)pyrrolidin-1-ium chloride (30). This compound was obtained from **29** employing similar methods as compound **10**. White solid; total yield 12% for 6 steps; purity 99.8%. ^{1}H NMR (400 MHz, DMSO-d_6) δ 9.30 (br s, 2H), 7.31 (t, J = 7.8 Hz, 2H), 7.02 (d, J = 8.3 Hz, 2H), 6.99 (t, J = 7.5 Hz, 1H), 6.41 (s, 1H), 5.17 (s, 2H), 4.29–4.13 (m, 2H), 3.33–3.26 (m, 1H), 3.25–3.17 (m, 1H), 3.18–3.07 (m, 1H), 3.06–2.90 (m, 1H), 2.84–2.65 (m, 1H), 2.19–1.95 (m, 1H), 1.84–1.62 (m, 1H). ^{13}C NMR (101 MHz, DMSO-d_6) δ 171.2, 169.0, 157.4, 129.6, 121.4, 114.7, 95.3, 70.3, 60.4, 46.5, 44.1, 36.6, 26.5. HRMS (ESI): calcd for $C_{15}H_{19}N_2O_3$ $[M+H]^+$, 275.1390; found, 275.1396.

***N*-(2-((5-(Phenoxymethyl)isoxazol-3-yl)oxy)ethyl)cyclopentanaminium chloride (36).** This compound was obtained from **33**, phenol, and cyclopentanone employed methods C, D1, F, and D1. White solid; yield 57% for the first two steps and 52% for the last two steps; purity 96.7%. ^{1}H NMR (400 MHz, DMSO-d_6) δ 9.35 (br s, 2H), 7.32 (t, J = 8.0 Hz, 2H, phenol), 7.12 – 6.91 (m, 3H, phenol), 6.44 (s, 1H, isoxazol), 5.20 (s, 2H, CH_2-O-phenol), 4.50 (t, J = 5.0 Hz, 2H, CH_2-O-isoxazol), 3.55–3.44 (m, 1H, cycloalkyl), 1.96 (d, J = 8.3 Hz, 2H, cycloalkyl), 1.7–1.62 (m, 4H, cycloalkyl), 1.56–1.47(m , 2H, cycloalkyl). ^{13}C NMR (101 MHz, DMSO-d_6) δ 170.8 (isoxazol), 169.2 (isoxazol), 157.4 (phenol), 129.6 (phenol), 121.4 (phenol), 114.7 (phenol), 95.4 (isoxazol), 65.5 (C-O-phenol), 60.4 (C-O-isoxazol), 58.6 (C-N-cycloalkyl), 44.6 (cycloalkyl), 28.9 (cycloalkyl), 23.6 (cycloalkyl). HRMS (ESI): calcd for $C_{17}H_{23}N_2O_3$ $[M+H]^+$, 303.1703; found, 303.1707. The interpretation of ^{1}H and ^{13}C NMR signals of **37-43** are similar with **36**.

***N*-(2-((5-(Phenoxymethyl)isoxazol-3-yl)oxy)ethyl)cyclohexanaminium chloride (37).** This compound was obtained from **33**, phenol, and cyclohexanone employed methods C, D1, F, and D1.

White solid; yield 49% for the first 2 steps and 54% for the last 2 steps; purity 96.5%. ^{1}H NMR (400 MHz, DMSO-d_6) δ 8.86 (br s, 2H), 7.41–7.23 (m, 2H), 7.10–6.89 (m, 3H), 6.39 (s, 1H), 5.17 (s, 2H), 4.28 (t, J = 6.0 Hz, 2H), 3.02 (t, J = 6.0 Hz, 2H), 2.16–2.07 (m, 2H), 2.07–1.97 (m, 2H), 1.82–1.71 (m, 2H), 1.64–1.55 (m, 1H), 1.38–1.16 (m, 4H). ^{13}C NMR (101 MHz, DMSO-d_6) δ 171.1, 169.0, 157.4, 129.6, 121.4, 114.7, 95.3, 67.0, 60.5, 55.9, 28.5, 25.4, 24.7, 23.8. HRMS (ESI): calcd for $C_{18}H_{25}N_2O_3$ $[M+H]^+$, 317.1860; found, 317.1845.

***N*-(2-((5-((3,4-Dichlorophenoxy)methyl)isoxazol-3-yl)oxy)ethyl)cyclohexanaminium chloride (38).** This compound was obtained from **33**, 3,4-dichlorophenol, and cyclohexanone employed methods C, D1, F, and D1. White solid; yield 49% for the first 2 steps and 53% for the last 2 steps; purity 99.2%. ^{1}H NMR (400 MHz, DMSO-d_6) δ 9.33 (br s, 2H), 7.57 (d, J = 9.0 Hz, 1H), 7.40 (d, J = 2.9 Hz, 1H), 7.08 (dd, J = 9.0, 3.0 Hz, 1H), 6.48 (s, 1H), 5.27 (s, 2H), 4.52 (t, J = 5.1 Hz, 2H), 3.34 (s, 2H), 3.02 (t, J = 9.4 Hz, 1H), 2.07 (dd, J = 12.4, 3.8 Hz, 2H), 1.76 (dt, J = 13.1, 3.4 Hz, 2H), 1.60 (dt, J = 12.5, 3.5 Hz, 1H), 1.42–1.30 (m, 2H), 1.30–1.15 (m, 2H), 1.15–1.06 (m, 1H). ^{13}C NMR (101 MHz, DMSO-d_6) δ 170.7, 168.3, 156.8, 131.6, 131.0, 123.4, 116.8, 115.8, 95.9, 65.5, 61.1, 56.3, 42.4, 28.2, 24.7, 23.9. HRMS (ESI): calcd for $C_{18}H_{23}Cl_2N_2O_3$ $[M+H]^+$, 385.1080; found, 385.1085.

***N*-(2-((5-((3-(Trifluoromethyl)phenoxy)methyl)isoxazol-3-yl)oxy)ethyl) cyclohexanaminium chloride (39).** This compound was obtained from **33**, 3-trifluoromethylphenol, and cyclopentanone employed methods C, D1, F, and D1. White solid; yield 42% for the first 2 steps and 45% for the last 2 steps; purity 98.8%. ^{1}H NMR (400 MHz, DMSO-d_6) δ 9.08 (br s, 2H), 7.56 (t, J = 7.60 Hz, 1H), 7.36 (d, J = 8.40 Hz, 3H), 6.47 (s, 1H), 5.31 (s, 2H), 4.63–4.40 (m, 2H), 3.01 (s, 2H), 2.11–1.98 (m, 2H), 1.82–1.70 (m, 2H), 1.70–1.54 (m, 1H), 1.45–1.03 (m, 6H). ^{13}C NMR (101 MHz, DMSO-d_6) δ 170.8, 168.7, 157.7, 130.9, 130.5 (q, $J_{C\text{-}F}$ = 30.9 Hz), 123.9 (q, $J_{C\text{-}F}$ = 273.7 Hz), 119.2, 118.1 (q, $J_{C\text{-}F}$

= 4.0 Hz), 111.5 (q, J_{C-F} = 4.0 Hz), 95.9, 65.6, 60.9, 56.4, 42.6, 28.4, 24.8, 24.0. HRMS (ESI): calcd for $C_{19}H_{24}F_3N_2O_3$ $[M+H]^+$, 385.1734; found, 385.1750.

***N*-Methyl-N-(2-((5-((3-(trifluoromethyl)phenoxy)methyl)isoxazol-3-yl)oxy)ethyl)cyclohexan-aminium chloride (40).** This compound was obtained from **34**, 3-trifluoromethylphenol, and cyclopentanone employed methods C, D1, F, and D1. Yellow oil; yield 41% for the first 2 steps and 40% for the last 2 steps; purity 98.8%. ^{1}H NMR (400 MHz, DMSO-d_6) δ 10.80 (br s, 1H), 7.57 (t, *J* = 7.9 Hz, 1H), 7.45 – 7.27 (m, 3H), 6.49 (s, 1H), 5.33 (s, 2H), 4.63 (dt, *J* = 10.4, 5.3 Hz, 2H), 3.69 – 3.53 (m, 1H), 3.43 (s, 1H), 3.23 (t, *J* = 11.9 Hz, 1H), 2.73 (s, 3H), 2.15 – 1.96 (m, 2H), 1.80 (d, *J* = 12.9 Hz, 2H), 1.60 (d, *J* = 12.8 Hz, 1H), 1.49–1.34 (m, 2H), 1.33–1.21 (m, 2H), 1.17–1.07 (m, 1H). ^{13}C NMR (101 MHz, DMSO-d_6) δ 170.6, 168.6, 157.7, 130.8, 130.3 (q, J_{C-F} = 31.6 Hz), 123.9 (q, J_{C-F} = 273.4 Hz), 119.1, 118.0 (q, J_{C-F} = 3.8 Hz), 111.4 (q, J_{C-F} = 3.8 Hz), 95.7, 64.7, 63.9, 60.8, 50.8, 45.2, 36.5, 26.2, 25.1, 24.6, 24.4. HRMS (ESI): calcd for $C_{20}H_{26}F_3N_2O_3$ $[M+H]^+$, 399.1890; found, 399.1890.

***N,N*-Dimethyl-4-(methyl(2-((5-(phenoxymethyl)isoxazol-3-yl)oxy)ethyl)amino)cyclohexane-1-carboxamide (42).** Compound **41** was obtained from **33**, phenol, and cyclopentanone employed methods C, D1, F, and D1 as crude product without purification. To a stirred solution of **41**(1.24 mmol) in 60 mL water/THF (1:1) was added NaOH (6.2 mmol) dropwise. After refluxing for 2 days, the mixture was diluted by EtOAc (50 mL) and washed with water (2×40 mL). The aqueous phase was acidified to pH 3-4 with 1N HCl and extracted by EtOAc (2×30 mL) again, then the combined organic layer was washed with brine (30 mL), dried over Na_2SO_4, concentrated in vaccum. To a solution of the residue, dimethylamine hydrochloride (0.8 mmol), and HATU (1.06 mmol) dissolved in DMF (20 mL) was added DIPEA (1.6 mmol) slowly at ice-water bath under Nitrogen. After

stirring 12 h at rt, the mixture was added 60 mL water, and then extracted by EtOAc (3×30 mL), the combined organic phase was washed with brine (50 mL), dried over Na_2SO_4, evaporated under vacuum and purified by flash chromatography to give the product **42**. Yellow oil; yield 50% for the first 2 steps and 32% for the last 3 steps; purity 98.8%. ^{1}H NMR (400 MHz, DMSO-d_6) δ 7.32 (td, *J* = 7.5, 1.9 Hz, 2H), 7.09–6.94 (m, 3H), 6.38 (s, 1H), 5.16 (s, 2H), 4.21 (dt, *J* = 12.1, 5.8 Hz, 2H), 2.99 (s, 3H), 2.86–2.73 (m, 5H), 2.42–2.33 (m, 1H), 2.23 (s, 3H), 1.86–1.67 (m, 4H), 1.49–1.20 (m, 5H). ^{13}C NMR (101 MHz, DMSO-d_6) δ 174.6, 171.3, 168.8, 157.4, 129.5, 121.4, 114.7, 95.4, 68.5, 61.8, 60.5, 51.8, 37.8, 36.7, 36.5, 34.9, 28.2, 26.9, 25.9, 24.6. HRMS (ESI): calcd for $C_{22}H_{32}N_3O_4$ $[M+H]^+$, 402.2387; found, 402.2399.

4-((Dimethylammonio)methyl)-*N*-methyl-*N*-(2-((5-(phenoxymethyl)isoxazol-3-yl)oxy)ethyl)cyclohexan-1-aminium chloride (43). To a suspension of $LiAlH_4$ (1.45 mmol) in anhydrous THF (20 mL) was added **42** (0.29 mmol) at ice-water bath with nitrogen protection. After stirring for 6 h at rt, the mixture was added 50 mL water, and then extracted by EtOAc (3×20 mL), the combined organic phase was washed with brine (50 mL), dried over Na_2SO_4, evaporated under vacuum and purified by flash chromatography to give the product **43**. Yellow solid; yield 80%; purity 99.3%. ^{1}H NMR (400 MHz, DMSO-d_6) δ 11.22–10.86 (m, 1H), 10.53 (br s, 1H), 7.39–7.27 (m, 2H), 7.10–6.95 (m, 3H), 6.46 (s, 1H), 5.20 (s, 2H), 4.74–4.54 (m, 2H), 3.73–3.57 (m, 1H), 3.51–3.41 (m, 1H), 3.32–3.22 (m, 1H), 3.20–3.13 (m, 1H), 2.98–2.85 (m, 1H), 2.82–2.64 (m, 9H), 2.19–2.10 (m, 1H), 2.08–1.98 (m, 1H), 1.95–1.84 (m, 2H), 1.83–1.42 (m, 4H), 1.12–0.93 (m, 1H). ^{13}C NMR (101 MHz, DMSO-d_6) δ 170.6, 169.2, 157.4, 129.6, 121.4, 114.7, 95.4, 64.6, 63.2, 60.4, 57.6, 50.9, 42.6, 42.4, 37.0, 36.5, 31.6, 28.5, 26.9, 25.8. HRMS (ESI): calcd for $C_{22}H_{34}N_3O_3$ $[M+H]^+$, 388.2595; found, 388.2611.

***tert*-Butyl (4-iodobutyl)carbamate (46).** This compound was obtained from **44** employing methods

A and B. Colorless oil; total yield 62% for 2 steps. ^{1}H NMR (400 MHz, $CDCl_3$) δ 4.74 (s, 1H, -NH), 3.20–3.16 (m, 4H, alkyl), 2.05–1.95 (m, 4H, alkyl), 1.42 (s, 9H, Boc). ^{13}C NMR (101 MHz, $CDCl_3$) δ 155.9 (C=O), 79.4 (C-O), 39.0 (alkyl), 30.5 (alkyl), 30.5 (alkyl), 28.3 (C_3-C-O), 5.2 (C-I). The interpretation of ^{1}H and ^{13}C NMR signals of **47** are similar with **46**.

***tert*-Butyl (6-iodohexyl)carbamate (47).** This compound was obtained from **45** employing methods A and B. Colorless oil; total yield 80% for 2 steps. ^{1}H NMR (400 MHz, $CDCl_3$) δ 4.74 (s, 1H), 3.20–3.16 (m, 4H), 1.93–1.83 (m, 4H), 1.42 (s, 9H), 1.33–1.20 (m, 4H). ^{13}C NMR (101 MHz, $CDCl_3$) δ 155.9, 79.4, 39.0, 31.7, 28.5, 28.3, 26.0, 25.5, 5.2.

***(2S)*-1-(6-Ammoniohexyl)-2-(((5-(phenoxymethyl)isoxazol-3-yl)oxy) methyl)pyrrolidin-1-ium chloride (48).** This compound was obtained from **10** and **47** employing method G and D1. Brown oil; total yield 23% for 2 steps; purity 95.4%; $[\alpha]_D^{20}$ = - 9.3 (*c* = 1 mg/mL, MeOH). ^{1}H NMR (400 MHz, D_2O) δ 7.25 (t, *J* = 7.8 Hz, 2H, phenol), 6.97 (d, *J* = 7.4 Hz, 1H, phenol), 6.91 (d, *J* = 8.0 Hz, 2H, phenol), 6.21 (s, 1H, isoxazol), 5.01 (s, 2H, CH_2-O-phenol), 4.53–4.30 (m, 2H, CH_2-O-isoxazol), 3.93–3.81 (m, 1H), 3.77–3.63 (m, 1H), 3.39–3.26 (m, 1H), 3.25–3.15 (m, 1H), 3.14–3.01 (m, 1H), 2.94 (t, *J* = 7.6 Hz, 2H), 2.36–2.22 (m, 1H), 2.19–2.07 (m, 1H), 2.07–1.95 (m, 1H), 1.94–1.82 (m, 1H), 1.76–1.56 (m, 4H), 1.43–1.27 (m, 4H). ^{13}C NMR (101 MHz, D_2O) δ 171.0 (isoxazol), 169.4 (isoxazol), 157.1 (phenol), 129.9 (phenol), 122.2 (phenol), 114.9 (phenol), 95.4 (isoxazol), 67.3 (C-O-phenol), 66.3 (C-O-isoxazol), 61.0 (pyrrolidin), 55.2 (alkyl), 54.9 (pyrrolidin), 39.3 (alkyl), 26.4, 25.8, 25.3, 25.1, 24.7, 22.2. HRMS (ESI): calcd for $C_{21}H_{32}N_3O_3$ $[M+H]^+$, 374.2438; found, 374.2425. The interpretation of ^{1}H and ^{13}C NMR signals of **49-51** are similar with **48**.

***(2S)*-1-(6-Ammoniohexyl)-2-(((5-((3-(trifluoromethyl)phenoxy)methyl)isoxazol-3-yl)oxy)methyl)pyrrolidin-1-ium chloride (49).** This compound was obtained from **16** and **47** employing methods

G and D. Brown oil; total yield 37% for 2 steps; purity 98.5%; $[\alpha]_D^{20}$ = -11 (*c* = 1 mg/mL, MeOH). ^{1}H NMR (400 MHz, DMSO-d_6) δ 11.00 (br s, 1H), 8.04 (br s, 3H), 7.57 (t, *J* = 8.0 Hz, 1H), 7.43–7.30 (m, 3H), 6.52 (s, 1H), 5.33 (s, 2H), 4.69 (dd, *J* = 11.5, 7.7 Hz, 1H), 4.50 (dd, *J* = 11.5, 3.9 Hz, 1H), 3.99–3.81 (m, 1H), 3.68–3.50 (m, 1H), 3.20–3.03 (m, 2H), 2.75 (q, *J* = 6.7 Hz, 2H), 2.32–2.11 (m, 1H), 2.07–1.93 (m, 2H), 1.87–1.70 (m, 2H), 1.68–1.24 (m, 8H). ^{13}C NMR (101 MHz, DMSO-d_6) δ 170.7, 168.6, 157.7, 130.8, 130.3 (q, $J_{C\text{-}F}$ = 31.9 Hz), 123.8 (q, $J_{C\text{-}F}$ = 273.5 Hz), 119.1, 118.0 (q, $J_{C\text{-}F}$ = 3.6 Hz), 111.4 (q, $J_{C\text{-}F}$ = 4.0 Hz), 95.7, 68.0, 65.3, 60.9, 54.1, 53.7, 38.4, 26.6, 26.5, 25.5, 25.3, 24.4, 21.8. HRMS (ESI): calcd for $C_{22}H_{31}F_3N_3O_3$ $[M+H]^+$, 442.2312; found, 442.2296.

***(2S)*-1-(6-Ammoniohexyl)-2-(((5-((3,4-dichlorophenoxy)methyl)isoxazol-3-yl)oxy)methyl)pyrrolidin-1-ium chloride (50).** This compound was obtained from **21** and **47** employing methods G and D. Brown oil; total yield 26% for 2 steps; purity 95.9%; $[\alpha]_D^{20}$ = - 10 (*c* = 1 mg/mL, MeOH). ^{1}H NMR (400 MHz, D_2O) δ 7.13 (d, *J* = 8.8 Hz, 1H), 6.84 (s, 1H), 6.68 (d, *J* = 8.6 Hz, 1H), 6.14 (br s, 1H), 4.90 (s, 2H), 4.45–4.25 (m, 2H), 3.87–3.74 (m, 1H), 3.69–3.57 (m, 1H), 3.25 (q, *J* = 10.6, 9.5 Hz, 1H), 3.12 (q, *J* = 7.9 Hz, 1H), 3.08–2.95 (m, 1H), 2.85 (t, *J* = 7.4 Hz, 2H), 2.30–2.13 (m, 1H), 2.12–1.99 (m, 1H), 1.98–1.89 (m, 2H), 1.88–1.76 (m, 1H), 1.70–1.46 (m, 4H), 1.33–1.17 (m, 4H). ^{13}C NMR (101 MHz, D_2O) δ 170.9, 168.6, 156.3, 132.2, 130.8, 124.4, 116.8, 114.7, 95.6, 67.4, 66.3, 61.4, 55.2, 54.8, 39.3, 26.4, 25.9, 25.3, 25.1, 24.7, 22.2. HRMS (ESI): calcd for $C_{21}H_{30}Cl_2N_2O_3$ $[M+H]^+$, 442.1659; found, 442.1653.

***(2S)*-1-(4-Ammoniobutyl)-2-(((5-((3,4-dichlorophenoxy)methyl)isoxazol-3-yl)oxy)methyl)pyrrolidin-1-ium chloride (51).** This compound was obtained from **21** and **46** employing methods G and D. Brown oil; yield 23% for 2 steps; purity 99.1%; $[\alpha]_D^{20}$ = - 13 (*c* = 1 mg/mL, MeOH). ^{1}H NMR (400 MHz, D_2O) δ 7.36 (d, *J* = 8.3 Hz, 1H), 7.12 (br s, 1H), 6.88 (d, *J* = 8.0 Hz, 1H), 6.24 (s, 1H), 5.09 (s,

2H), 4.61–4.29 (m, 2H), 4.06–3.86 (m, 1H), 3.79–3.60 (m, 1H), 3.54–3.31 (m, 1H), 3.33–3.06 (m, 2H), 3.07–2.83 (m, 2H), 2.37–2.19 (m, 1H), 2.19–2.06 (m, 1H), 2.08–1.88 (m, 2H), 1.87–1.52 (m, 4H). ^{13}C NMR (101 MHz, D_2O) δ 171.1, 169.1, 156.3, 132.3, 130.9, 124.7, 117.0, 115.2, 95.5, 67.3, 66.7, 61.6, 54.9, 54.4, 38.8, 25.8, 24.0, 22.2, 22.2. HRMS (ESI): calcd for $C_{19}H_{26}Cl_2N_3O_3$ $[M+H]^+$, 414.1346; found, 414.1363.

In Vitro Binding Studies. Radioligand competition studies were carried out by the National Institute of Mental Health's Psychoactive Drug Screening Program. For experimental details please refer to the PDSP ASSAY PROTOCOL BOOK III, on the Web site http://pdsp.med.unc.edu/.

Cell Culture. Two osteosarcoma cell lines and three normal cell lines were used in this study: 143B, MOS-J, LO2, HaCaT and HAF. 143B, LO2, HaCaT, and HAF cells were maintained in DMEM (GIBICO) supplemented with L-glutamine (2 mM); MOS-J in αMEM (GIBICO). All medium were supplemented with 1% penicillin/ streptomycin (Hyclone) and 10% fetal bovine serum (GIBICO). The cells were incubated in a humidified atmosphere of 5% CO_2/95% air at 37 ℃.

Cytotoxicity Assay and Growth Curve Assay. Cell viability/cytotoxicity was measured by crystal violet assay method. 1,000 cells were seeded in each well of 96-well plates. Incubate the cells for 24 h at 37 ˚C to enable adhesion of cells to wells. Replace medium supplemented with σ2 ligand appropriate for the experimental goals. After 48 h, cells were fixed with 4% paraformaldehyde (PFA) for 30 min or longer, and then stained with 0.1% crystal violet for 20 min. Wash the cells with double distilled water by 5 times. The plates were drained on paper towels to complete dry. The stain can be

solubilized in 100uL 33% glacial acetic acid, shake until color is uniform the read the absorbance of each at 570 nm. The p value was calculated by paired t test.

Apoptosis Detection by Flow Cytometry for Annexin-V. Cells were seeded into 6-well plates and the following day treated with σ2 ligand (5 μM) or DMSO. After 12 h the cells were assayed using the Annexin-V FITC Kit (Invitrogen). The cells were prepared as directed by the manufacturer and then, analyzed with a FACS Fortessa flow cytometer (BD Biosciences).

Cell Cycle Analysis. Cells were cultured in a 6-well plate and, 12 h seeding treated with σ2 ligands (5 μM) after. After incubation of 24 h, the cells were harvested, fixed in ethanol (80%) and stained with propidium iodide (50 μg/mL). RNase was used to degradate RNA in cells before staining. And after staining, the prepared cells were analyzed with a FACS Fortessa flow cytometer (BD Biosciences). The percentage of cells residing in different phases of cell cycle was compared with control.

Clonogenic Assay. 143B cells were plated at a density of 1000 cells per well in 6-well plates. After 24 h of adhesion, cells were treated with σ2 ligand or DMSO at appropriate density for the experimental goals. The culture medium was changed every 2 days. Colonies were cultured for 10 days, and then we removed the medium washed the cell with PBS by 2 times and fixed the cells with 4% PFA. Cells were stained with 0.1% crystal violet for 20 min. Wash the cells with double distilled H_2O by 5 times. Dry the plates and take photos by microscopy (OLYMPUS). Colonies that contained 50 or more cells were counted.

ACKNOWLEDGMENTS

This work was supported by grants from the National Natural Science Foundation of China (81402780 to LF. Y., 81722020 and 8171101485 to J. L.), the National Key Research and Development Program of China (2018YFC1105102 to J. L.). We thank the PDSP for performing binding affinity assays for σ2. We thank Jiangsu Nhwa Pharmaceutical Co., Ltd. for performing binding affinity assays for σ1.

Reference

[1] W. R. Martin, C. G. Eades, J. A. Thompson, R. E. Huppler, P. E. Gilbert, *J. Pharmacol. Exp. Ther* **1976**, *197*, 517–532.

[2] N. Khazan, G. A. Young, E. E. El-Fakany, O. Hong, D. Calligaro, *Neuropharmacology* **1984**, *23*, 983-987.

[3] W. D. Bowen, *Pharm. Acta Helv* **2000**, *74*, 211-218.

[4] R. Quirion, W. D. Bowen, Y. Itzhak, J. L. Junien, J. M. Musacchio, R. B. Rothman, T. P. Su, S. W. Tarm, D. P. Taylor, *Trends Pharmacol. Sci.* **1992**, *113*, 85-86.

[5] a, R. H. Mach, C. Zeng, W. G. Hawkins, *J Med Chem* **2013**, *56*, 7137-7160; b, T. Hayashi, *Journal of pharmacological sciences* **2015**, *127*(1), 2-5.

[6] M. Hanner, F. F. Moebius, A. Flandorfer, H. G. Knaus, J. Striessnig, E. Kempner, H. Glossmann, *P. Natl. Acad. Sci. USA* **1996**, *93*, 8072-8077.

[7] H. R. Schmidt, S. Zheng, E. Gurpinar, A. Koehl, A. Manglik, A. C. Kruse, *Nature* **2016**, *532*, 527-530.

[8] T. P. Su, T. C. Su, Y. Nakamura, S. Y. Tsai, *Trends Pharmacol. Sci.* **2016**, *37*, 262-278.

[9] a, T. Hayashi, T. P. Su, *Cell* **2007**, *131*, 596-610; b, T. Hayashi, T. P. Su, *P. Natl. Acad. Sci. USA* **2001**, *98*, 491-496.

[10] M. Fujimoto, T. Hayashi, R. Urfer, S. Mita, T. P. SU, *SYNAPSE* **2012**, *66*, 630-639.

[11] J. S. James, L. M. Galo, R. R. Pradipta, F. M. Stephen, J. P. Theodore, *ACS Chem. Neurosci* **2017**, *8*, 1801-1811.

[12] S. B. Hellewell, W. D. Bowen, *Brain Res.* **1990**, *527*, 244-253.

[13] aS. B. Hellewell, A. Bruce, G. Feinstein, J. Orringer, W. Williams, W. D. Bowen, *Eur. J. Pharmacol.* **1994**, *268*, 9-18; bK. T. Wheeler, L. Wang, C. A. Wallen, S. R. Childers, J. M. Cline, P. C. Keng, R. H. Mach, *Br J Cancer* **2000**, *82*, 1223-1232.

[14] N. A. Colabufo, F. Berardi, C. Abate, M. Contino, M. Niso, R. Perrone, *J Med Chem* **2006**, *49*, 4153-4158.

[15] J. J. Peluso, X. Liu, A. Gawkowska, V. Lodde, C. A. Wu, *Mol. Cell. Endocrinol* **2010**, *320*, 153-161.

[16] J. Xu, C. Zeng, W. Chu, F. Pan, J. M. Rothfuss, F. Zhang, Z. Tu, D. Zhou, D. Zeng, S. Vangveravong, F. Johnston, D. Spitzer, K. C. Chang, R. S. Hotchkiss, W. G. Hawkins, K. T. Wheeler, R. H. Mach, *Nat. Commun.* **2011**, *2*, 380.

[17] a, C. Abate, M. Niso, V. Infantino, A. Menga, F. Berardi, *Eur. J. Pharmacol.* **2015**, *758*, 16-23; b, M. L. Pati, D. Groza, C. Riganti, J. Kopecka, M. Niso, F. Berardi, S. Hager, P. Heffeter, M. Hirai, H. Tsugawa, Y. Kabe, M. Suematsu, C. Abate, *Pharmacol. Res.* **2017**, *117*, 67-74.

[18] A. Alon, H. R. Schmidt, M. D. Wood, J. J. Sahn, S. F. Martin, A. C. Kruse, *P. Natl. Acad. Sci. USA* **2017**, *114*, 7160-7165.

[19] a, J. R. Hornick, S. Vangveravong, D. Spitzer, C. Abate, F. Berardi, P. Goedegebuure, R. H. Mach, W. G. Hawkins, *J. Exp. Clin. Cancer Res.* **2012**, *31*, 41; b, H. Kashiwagi, J. E. McDunn, P. O. S. Jr, P. S. Goedegebuure, S. Vangveravong, K. Chang, R.

S. Hotchkiss, R. H. Mach, W. G. Hawkins, *J Transl Med* **2009**, *7*, 24; c, M. L. Pati, M. Niso, D. Spitzer, F. Berardi, M. Contino, C. Riganti, W. G. Hawkins, C. Abate, *Eur. J. Med. Chem* **2018**, *144*, 359-371; d, C. Abate, R. Perrone, F. Berardi, *Curr. Pharm. Design* **2012**, *18*, 938-949; e, Y. S. Huang, H. L. Lu, L. J. Zhang, Z. Wu, *Med. Res. Rev.* **2014**, *34*, 532-566; f, M. Niso, C. Abate, M. Contino, S. Ferorelli, A. Azzariti, R. Perrone, N. A. Colabufo, F. Berardi, *ChemMedChem* **2013**, *8*, 2026-2035; g, S. Franchini, C. Sorbi, U. M. Battisti, A. Tait, L. I. Bencheva, E. Cichero, P. Fossa, A. Cilia, O. Prezzavento, S. Ronsisvalle, G. Arick, L. Benassi, C. Vaschieri, P. Azzoni, C. Magnoni, L. Brasili, *ChemMedChem* **2017**, *12*, 1893-1905; h, H. Nicholson, A. Comeau, C. Mesangeau, C. R. McCurdy, W. D. Bowen, *J. Pharmacol. Exp. Ther* **2015**, *354*, 203-212; i, A. Tesei, M. Cortesi, A. Zamagni, C. Arienti, S. Pignatta, M. Zanoni, M. Paolillo, D. Curti, M. Rui, D. Rossi, S. Collina, *Front. Pharmacol* **2018**, *9*, 711.

[20] M. L. Pati, J. R. Hornick, M. Niso, F. Berardi, D. Spitzer, C. Abate, W. Hawkins, *BMC Cancer* **2017**, *17*, 51.

[21] G. Romeo, O. Prezzavento, S. Intagliata, V. Pittala, M. N. Modica, A. Marrazzo, R. Turnaturi, C. Parenti, S. Chiechio, E. Arena, A. Campisi, G. Sposito, L. Salerno, *Eur. J. Med. Chem* **2019**, *174*, 226-235.

[22] C. Zeng, S. Vangveravong, J. Xu, K. C. Chang, R. S. Hotchkiss, K. T. Wheeler, D. Shen, Z. P. Zhuang, H. F. Kung, R. H. Mach, *Cancer Res* **2007**, *67*, 6708-6716.

[23] a, M. Rui, D. Rossi, A. Marra, M. Paolillo, S. Schinelli, D. Curti, A. Tesei, M. Cortesi, A. Zamagni, E. Laurini, S. Pricl, D. Schepmann, B. Wunsch, E. Urban, V. Pace, S. Collina, *Eur. J. Med. Chem* **2016**, *124*, 649-665; b, C. Zeng, J. Rothfuss, J. Zhang, W. Chu, S. Vangveravong, Z. Tu, F. Pan, K. C. Chang, R. Hotchkiss, R. H. Mach, *Br. J. Cancer* **2012**, *106*, 693-701.

[24] a, D. Li, Y. Chen, X. Wang, W. Deuther-Conrad, X. Chen, B. Jia, C. Dong, J. Steinbach, P. Brust, B. Liu, H. Jia, *J. Med. Chem* **2016**, *59*, 934-946; b, C. Zeng, S. Vangveravong, L. A. Jones, K. Hyrc, K. C. Chang, J. Xu, J. M. Rothfuss, M. P. Goldberg, R. S. Hotchkiss, R. H. Mach, *Mol. Imaging* **2011**, *10*, 420-433; c, M. L. Pati, E. Fanizza, S. Hager, D. Groza, P. Heffeter, A. G. Laurenza, V. Laquintana, M. L. Curri, N. Depalo, C. Abate, N. Denora, *Mol. Pharm* **2018**, *15*, 458-471; d, F. Dehdashti, R. Laforest, F. Gao, K. I. Shoghi, R. L. Aft, B. Nussenbaum, F. H. Kreisel, N. L. Bartlett, A. Cashen, N. Wagner-Johnson, R. H. Mach, *J. Nucl. Med* **2013**, *54*, 350-357.

[25] J. R. Hornick, J. Xu, S. Vangveravong, Z. Tu, J. B. Mitchem, D. Spitzer, P. Goedegebuure, R. H. Mach, W. G. Hawkins, *Mol. Cancer* **2010**, *9*, 298.

[26] a, D. Spitzer, P. O. Simon, H. Kashiwagi, J. Xu, C. Zeng, S. Vangveravong, D. Zhou, K. Chang, J. E. McDunn, J. R. Hornick, P. Goedegebuure, R. S. Hotchkiss, R. H. Mach, W. G. Hawkins, *Cancer Res* **2012**, *72*, 201-209; b, Y. Zhang, Y. Huang, P. Zhang, X. Gao, R. B. Gibbs, S. Li, *Int. J. Nanomed* **2012**, *7*, 4473-4485.

[27] a, H. E. Nicholson, W. F. Alsharif, A. B. Comeau, C. Mesangeau, S. Intagliata, M. Mottinelli, C. R. McCurdy, W. D. Bowen, *J. Pharmacol. Exp. Ther.* **2019**, *368*, 272-281; b, S. Intagliata, W. F. Alsharif, C. Mesangeau, N.Fazio, M. Seminerio, Y. T. Xu, R. R. Matsumoto, C. R. McCurdy, *Euro. J. Med. Chem* **2019**, *165*, 250-257.

[28] L. F. Yu, H. K. Zhang, H. Gunosewoyo, A. P. Kozikowski, *ACS Med. Chem. Lett.* **2012**, *3*, 1054-1058.

[29] H. Sun, M. Shi, W. Zhang, Y. M. Zheng, Y. Z. Xu, J. J. Shi, T. Liu, H. Gunosewoyo, T. Pang, Z. B. Gao, F. Yang, J. Tang, L. F. Yu, *J. Med. Chem.* **2016**, *59*, 6329−6343.

[30] H. Sun, Y. J. Wang, W. W. Shi, F. Yang, J. Tang, T. Pang, L. F. Yu, *RSC Adv.* **2018**, *8*, 7080-7088.

[31] a, L. Mirabello, R. J. Troisi, S. A. Savage, *Cancer* **2009**, *115*, 1531-1543; b, K. A. Janeway, D. A. Barkauskas, M. D. Krailo, P. A. Meyers, C. L. Schwartz, D. H. Ebb, N. L. Seibel, H. E. Grier, R. Gorlick, N. Marina, *Cancer* **2012**, *118*, 4597-4605; c, J. PosthumaDeBoer, M. A. Witlox, G. J. L. Kaspers, B. J. V. Royen, *Clin. Exp. Metastasis* **2011**, *28*, 493–503.

[32] a, G. Bacci, S. Ferrari, F. Bertoni, P. Ruggieri, P. Picci, A. Longhi, M. Campanacci, *J Clin Oncol* **2000**, *18*, 4016–4027; b, L. Kager, A. Zoubek, U. Potschger, U. Kastner, S. Flege, B. Kempf-Bielack, G. Jundt, *J Clin Oncol* **2003**, *21*, 2011–2018.

[33] V. Mialou, T. Philip, C. Kalifa, D. Perol, J. C. Gentet, P. Marec-Berard, O. Hartmann, *Cancer* **2005**, *104*, 1100–1109.

[34] a, A. Deshpande, P. W. Hinds, *Curr Mol Med* **2006**, *6*, 809–817; b, N. Gokgoz, J. S. Wunder, S. Mousses, S. Eskandarian, R. S. Bell, I. L. Andrulis, *Cancer* **2001**, *92*, 2181–2189; c, M. Overholtzer, P. H. Rao, R. Favis, X. Y. Lu, M. B. Elowitz, F. Barany, A. J. Levine, *P. Natl. Acad. Sci. USA* **2003**, *100*, 11547–11552.

[35] D. S. Geller, R. Gorlick, *Clin. Adv. Hematol. Oncol* **2010**, *8*, 705–718.

[36] N. A. Franken, H. M. Rodermond, J. Stap, J. Haveman, C. van Bree, *Nat Protoc* **2006**, *1*(5), 2315-2319.